UNIVERSITÄTSKLINIKUM HAMBURG-EPPENDORF

Institut für Tumorbiologie

Prof. Dr. med. Klaus Pantel

Investigating the role of tyrosine-protein kinase MER in human breast cancer

Dissertation

zur Erlangung des Grades eines Doktors der Medizin
an der Medizinischen Fakultät der Universität Hamburg.

vorgelegt von:

Mathias Meng Xiao Jahn Yuan
aus Aachen

Hamburg 2023

Angenommen von der
Medizinischen Fakultät der Universität Hamburg am: 04.03.2024

Veröffentlicht mit Genehmigung der
Medizinischen Fakultät der Universität Hamburg.

Prüfungsausschuss, der/die Vorsitzende: PD Dr. Andreas Block

Prüfungsausschuss, zweite/r Gutachter/in: Prof. Dr. Klaus Pantel

1 Table of Contents

1 List of Tables

2 List of Figures

3 Introduction

3.1 Breast cancer

“Ars longa, vita brevis – Art is long, life is short” said the Greek physician Hippocrates. Medicine, the art of understanding health and disease, is in a constant tuck of war with the finiteness of life. Yet cancer, the “Emperor of all Maladies” as S. Mukherjee regarded it as (Mukherjee, 2010), first described as early as 1600 BC (Hajdu, 2011), accompanies life like no other. Cancer is a disease in which abnormal cells proliferate uncontrolled and form tumors that can spread within the body to distant sites to form metastasis. It is the second leading cause of death globally, accounting for an estimated 9.9 million deaths in 2020 (Ferlay et al., 2021). One out of three people will develop cancer in their lifetime (Howlader, 2016). With respect to its significant medical, social, and economic implications, cancer poses a global challenge for us now and in the future.

Breast cancer alone is the most common cancer in women and the second most common type of cancer overall (World-Cancer-Research-Fund, 2018). Over 2 million new cases were reported in 2018, corresponding to a prevalence in women of 665 per 100,000 in Western Europe (Ferlay J, 2012). Breast cancer can be classified according to its tissue invasiveness. The non-invasive type is called “in situ carcinoma”, which has a comparably good prognosis. Once a tumor has crossed the basal membrane, it has invaded and is therefore called “invasive carcinoma”. Histologically invasive carcinoma can be subdivided into no-special-type (75% of all tumors of the breast) or special types (25%) such as lobular, tubular, cribriform, inflammatory, etc.

3.1.1 Molecular determinants of malignancy

With growing advancements in science, cellular and molecular differences in breast cancers have been observed, which greatly improved the range of therapeutic strategies and outcomes. Most patients have tumors in which hormone receptors (HR) for estrogen and progesterone (ER, PR) are overexpressed. These are classified as “luminal A”.

“Luminal B” tumors are either ER/PR positive and human epidermal growth factor receptor 2 (HER2) positive, or they are HER2 negative but Ki67 index high. A high Ki67 index is an immunohistochemically determined cell proliferation associated with fast-growing tumors and poor prognosis. A tumor that is HER2-positive only is classed as “HER2-enriched”. “Triple-negative” breast cancers (TNBC) do not express any ER, PR or HER2 and histologically often resemble the basal cells surrounding the mammary gland's ductal cells. With decreasing trend, luminal A breast cancer has the best prognosis, while TNBC exhibits the worst. Efficient therapeutic targeting of hormone receptors is partially responsible for the markedly different outcomes between these subtypes. Consistently, TNBC has a worse prognosis due to its high aggressiveness and proliferation rate and lack of therapeutically targetable high-frequency driver alterations (e.g., ER, PR, HER2) (Shaver et al., 2016). Lastly, the “normal-like” subtype resembles the “luminal A” expression profile but has a slightly worse prognosis than “luminal A” cancer prognosis.

Table 1 | Molecular classification of Human Breast Cancer

Molecular Subtype		**HR**	**HER2**	**Ki67**
Luminal A		positive	negative	low
Luminal B	HER2 negative	positive	negative	high
	HER2 positive	positive	positive	Any value
HER2 enriched		negative	positive	Any value
Triple negative		negative	negative	Any value
Normal-like		positive	negative	low

(Geyer et al., 2009)

In addition to these markers, further research has utilized genome-based methods such as next-generation sequencing to define prognostic and therapeutic molecular markers that allow the transition into the patient-based precision medicine (Tsang and Tse, 2020, Vuong et al., 2014)

3.1.2 Current standard treatment

According to the Union for International Cancer Control (UICC) and American Joint Commission on Cancer (AJCC), the therapeutic approach to breast cancer is based on the molecular subtype and its cancer staging of the tumor. Stage I tumors are smaller than 2 cm, and no axillary lymph nodes or metastasis can be detected. In stage II axillary lymph nodes are affected, or the tumor size exceeds 5 cm. In stage III, tumors spread to extended axillary lymph nodes or the lymph nodes near the arteria mammary interna regardless of the tumor size and infiltration. Stage IV tumors have already formed “distant metastasis” in non-regional lymph nodes or other organs such as bones, lungs, liver, and brain. With increasing stage, the 5-year relative survival decreases from 80-90 % at stage I/II to 24 % at stage III/IV (American-Cancer-Society, 2019). If metastasis has not been detected (stage I – III), a curative approach that aims to kill all cancer cells is indicated. In case of detected metastasis (stage IV), the therapy has a palliative approach that focuses on prolonging and advancing the quality of the life of the patient. Treatment details may differ according to different guidelines. Several treatment modalities can be chosen singularly or in combination.

With the goal of complete resection of the tumor, surgery is performed either in a breast-conserving manner or in a mastectomy, the removal of the entire breast tissue. Breast conservation therapy started > 30 years ago and is applicable to 60 - 80% of newly diagnosed breast cancers in Western Europe (Senkus et al., 2015). Mastectomy can be chosen depending on the tumor, e.g., large size, multicentricity, low margins to healthy tissue or patient choice. During surgery, axillary lymph nodes are also removed for diagnostic purposes and therapeutic effects. The number of nodes removed depends on the spread of cancer which is usually determined histopathologically during surgery.

Systemic therapy with pharmacological agents can either be given prior to surgery, a method termed neo-adjuvant, or after surgery, i.e., adjuvant. Factors that are primarily considered hereby are operability, type of cancer and UICC stage. The standard chemotherapy regimen is the combination of an anthracycline- and a taxane-type substance over a period of 18-24 weeks.

Furthermore, endocrine therapy is effective in Luminal A and B subtypes and contains the following substance groups: aromatase inhibitors, selective estrogen-receptor-modulators and gonadotropin-releasing hormone analogs. Those substances either decrease hormone production or block the hormone receptor. A more novel approach to systemic therapy is the administration of monoclonal antibodies (mAbs). Trastuzumab and pertuzumab, both selective mAbs against HER2, have proven to be very effective in HER2-enriched tumors and are given in combination with chemotherapy in metastatic state. Finally, CDK4/6 inhibitors which suppress the activity of cell-cycle regulating kinases, can also be utilized in systemic therapy.

Radiation therapy of the breast, chest wall and axilla can be administered in order to decrease the risk of relapse and metastasis. A fractionated dosage of e.g. 40-50 Gy for the remaining breast tissue is usually given over 3-6 weeks. Of note, after a breast-conserving surgery, radiation therapy is in most cases obligatory. Based on the spread into lymph nodes, radiation of lymphatic vessels may also be indicated.

3.1.3 Metastasis

Metastasis is the growth of cancer cells that have spread from the primary tumor to distant sites. It is still the leading cause of cancer-related death, despite the wide range of therapies for treating cancer, including pharmacology, radiation and surgery. Single cells can resist treatment and spread to form new metastasis. Stephen Paget, an English surgeon, first discovered that every tumor type has a specific tendency to migrate into preferred organs. Thus, he developed a theory that metastasis depends on the interaction between the cancer cell (the “seed”) and its specific tissue microenvironment (the “soil”) (Paget, 1889). This “seed and soil” model still holds true today and underlines the importance of the tumor microenvironment (see section 3.1.4) in metastasis. In breast cancer, the most common sites of metastasis are the lungs, liver and bone (Weigelt et al., 2005, Chiang and Massagué, 2008).

The development of metastases is a multi-step process that involves many intracellular and intercellular molecular changes. In brief, tumor cells invade the surrounding tissue, detach from their cell colony, find an entry into lymphatic or blood vessels - a process called intravasation - survive during hematogenous transit, arrest at a new location and exit into the tissue by extravasation at the distant site and form a new cell colony that grows to a clinically detectable size (Fidler, 2003).

Cancer cells must first undergo epithelial-mesenchymal-transition (EMT), a process in which the properties of an epithelial cell change and allow the cell to appear as a mesenchymal cell. During this progression, cancer cells need to acquire different functions and adapt to changing environments. Especially increased cell motility, invasion, resistance to apoptosis and extracellular degradation ability are the most notable among the newly acquired functions after EMT. The dissemination process continues with the detachment from surrounding cells and invasion through the basement membrane that lies at the basal side of epithelial cells. This entire process is driven by EMT-activating transcription factors, mainly of the SNAIL, TWIST and ZEB families (Brabletz et al., 2018). They also affect the composition of the tumor microenvironment (see section 3.1.4) by influencing the expression of tumor-promoting cytokines (Jing et al., 2011).

Apart from the aforementioned metastatic steps, the metastatic process has been refined further. Characteristics such as adapting to supportive niches, evading tissue defenses against infiltration as well as newly characterized survival pathways and therapy evading mechaisms have been further described (Massague and Obenauf, 2016). With the use of genomic data,

certain pro-metastatic genes have been found (Reiter et al., 2018, Hu et al., 2020, Ganesh and Massague, 2021). Interestingly, cancer treatment applies further selection pressure to metastatic cells and changes the genetical mutations in relapsed disease (Nguyen et al., 2009)

In order to investigate the molecular mechanisms driving metastasis, a suitable *in vivo* model is required. To model metastasis in murine models, the laboratory by Prof. Tavazoie at the *Rockefeller University* utilized an *in vivo* selection model that Isaiah Fidler and colleagues initially developed to generate metastatic mouse tumor cell lines. In this model, human TNBC breast cancer cells (MDA-MB-231) are injected into the circulation of an immunodeficient mouse. After lung metastases are detected, these are extracted, dissociated and re-injected into another mouse. This process is repeated several times to select *in vivo* for specific cells with the capability to successfully metastasize the lungs. Afterward, this generated subline (MDA-LM2) can be compared to its poorly metastatic parental cell line to identify molecular traits that promote metastasis (Tavazoie et al., 2008, Png et al., 2011, Minn et al., 2005).

3.1.4 Tumor microenvironment

It has been observed in mammographic imaging that breast tissue density positively correlates with up to 6-fold increased risk for breast cancer (Boyd et al., 2002, Boyd et al., 2011) and that tumors arise in the denser part of the breast tissue (Li et al., 2005, Ursin et al., 2005). This led to the investigation of the tumor microenvironment (often referred to as the tumor stroma), which applies to the complex of cancer cells and the surrounding non-cancerous cells and structures in the tumor. Components of the microenvironment include immune cells, endothelial cells, fibroblasts, adipocytes, extracellular matrix and various cytokines. In close interaction between cancer cells and their microenvironment, tumors create favorable environments for the growth and spread of cancer cells.

Tumor cells require blood vessels to receive nutrients and performing intravasation. Angiogenesis, the formation of new blood vessels from pre-existing vessels, is a physiological as well as tumor–initiated process. Tumors do not grow larger than 2 mm without new vessels (Longatto Filho et al., 2010). Microvessel density (MVD) correlates with a worse cancer prognosis (Linderholm et al., 2000) and metastatic capability (Png et al., 2011) in breast cancer. Most notably, the vascular endothelial growth factor (VEGF) is being implicated as the signal to attract endothelial cells towards cancer cells to promote intravasation.

After intravasation, circulating tumor cells (CTCs) can be found as single cells or in multicellular clusters and may seed metastasis at distant sites (Joosse et al., 2015). These cell clusters have been found to travel through capillaries as a single-chain (Au et al., 2016). Studies show that CTCs in clusters possess a higher efficiency than single CTCs in metastatic colonization, mainly due to their advantage in resisting apoptosis (Aceto et al., 2014). After cells arrive at a distant site, mesenchymal-epithelial-transition (MET), the reverse process of EMT, is likely due to the lack of EMT-stimulating factors present in the primary tumor microenvironment. MET is also considered a requirement for the secondary tumor formation (Kalluri and Weinberg, 2009). Eventually, less than 0.01% of CTCs can successfully form a secondary tumor (Chambers et al., 2002, Yoshida et al., 1993). Common reasons for this low efficiency are an arduous journey through the vasculature, death by immune cells, and failure to create a growth-promoting tumor microenvironment at the distal site. Furthermore, the lack of angiogenesis and cancer cells going into dormancy, a state of arrested growth, are limiting factors for metastatic growth (Lambert et al., 2017).

3.2 MERTK - Mer tyrosine kinase

3.2.1 Discovery

Receptor tyrosine kinases are cell-surface transmembrane proteins with a protein tyrosine kinase within their cytoplasmic domain (Lemke and Rothlin, 2008). They regulate vast amounts of intracellular signal pathways. Importantly, RTKs are often dysregulated by mutations or abnormal expression in cancer (Du and Lovly, 2018).

Myeloid-epithelial-reproductive tyrosine kinase (MERTK) is an RTK, which together with TYRO3 and AXL (Prasad et al., 2006) belongs to the TAM receptor family. PCR analysis identified the TAM group as a distinct protein tyrosine kinase group (Lai and Lemke, 1991). MERTK was identified first in the cancer context in a human glioblastoma library and was given its name after its expression in monocytes, epithelial and reproductive cells (Graham et al., 1994). MERTK expression was also detected in hematological cells, particularly macrophages, dendritic cells, natural killer (NK) cells, NK-T-cells, megakaryocytes, and platelets (Graham et al., 1994, Angelillo-Scherrer et al., 2001, Behrens et al., 2003). High levels of MERTK expression are also found in the ovary, prostate, testis, lung, retina, and kidney (Graham et al., 1994).

MERTK has an extracellular, transmembrane and intracellular component. The extracellular domain functions as a ligand binding site. It has also been described that the extracellular domain can be enzymatically cleaved by the metalloproteinase ADAM17 (Thorp et al., 2011). The soluble MERTK (sMER) can subsequently act as a ligand trap (Sather et al., 2007, Png et al., 2011, Nguyen et al., 2014). The intracellular domain contains the tyrosine kinase domain. Following ligand binding, MERTK dimerizes and autophosphorylates at three tyrosine residues within the kinase domain (Ling et al., 1996). Numerous proteins downstream of MERTK can affect cell proliferation, survival, transcription and migration. The MAPK/ERK and PI3K/AKT pathways are best described in multiple cancer entities (Linger et al., 2008, Hill, 2015, Jiang et al., 2019, Azad et al., 2020, Yan et al., 2018). It has been observed that receptor activation using antibodies reduces expression on the surface by receptor internalization and degradation (Cummings et al., 2014). Whether this process takes place by clathrin-mediated endocytosis remains under investigation. Functionally, internalization ensures functional downregulation by transporting MERTK into lysosomes for degradation and/or receptor transportation to the nucleus (Cummings et al., 2014). In support of the latter function, a nuclear localization sequence was identified in MERTK, but a specific function of MERTK in the nucleus remains to be determined. (Migdall-Wilson et al., 2012).

3.2.2 Receptor Ligands

MERTK is activated by the binding of its extracellular ligands Protein S (Pros1) and Growth arrest-specific 6 (Gas6) (Ohashi et al., 1995, Nagata et al., 1996, Tn Stitt et al., 1995, Mark et al., 1996), tubby, tubby-like protein 1 (TULP1) and Galectin-3 (Caberoy et al., 2010, Caberoy et al., 2012). The latter three ligands have been identified more recently and their interactions are still poorly characterized. Although Gas6 and Pros1 share a protein structure overlap by ~42%, they function differently in the human organism. These ligands bind via their C-terminal laminin G regions in the sex hormone binding globulin domain (SHBG) to the extracellular N-terminal immunoglobulin-like domains of MERTK. Following binding, dimerization of both the ligands and MERTK occur (Uehara and Shacter, 2008, Lemke and Rothlin, 2008).

The function of Pros1 is best characterized in anti-coagulation, in which it works as a co-factor for Protein C, an antagonist of factors Va and VIIIa in the coagulation cascade. In the cancer

context, higher expression of Pros1is associated with poor prognosis in the prostate (Saraon et al., 2012), thyroid (Wang et al., 2021) and oral squamous cell carcinoma (Abboud-Jarrous et al., 2017). Gas6, on the other hand, is only known to bind to TAM receptors. Several cancer entities are linked to Gas6 overexpression including colon, thyroid, breast, lung carcinomas, ovarian cancer and others (reviewed in Wu, 2017). Both Gas6 and Pros1 also act as bridging molecules between apoptotic cells (AC) and MERTK on phagocytic macrophages. Furthermore, Gas6 is secreted in an autocrine/paracrine manner in immune cells for anti-inflammatory polarization (Zizzo et al., 2012).

3.2.3 Function

The physiology of MERTK has been studied extensively after the successful generation of the *Tyro3* $^{-/-}$ *Axl* $^{-/-}$ *Mertk* $^{-/-}$ triple-knock-out (TAM TKO) mouse model (Lu et al., 1999). At birth TAM TKO mice show no phenotypic difference to the wildtype. However, at the age of 2-3 weeks, several degenerative phenotypes develop in the reproductive, retinal and hematopoietic systems (Lemke and Burstyn-Cohen, 2010) that resemble autoimmune-like symptoms. Histologically, accumulations of apoptotic cells, hyperactivation of APCs (Lu et al., 1999, Scott et al., 2001) and increased inflammation with autoantibody production in the entire body are found. These phenotypes are present but less pronounced in *Mertk* $^{-/-}$ animals due to the partially redundant function of TAM receptors (Lu et al., 1999). The *Mertk* $^{-/-}$ mouse shows Retinitis pigmentosa as a consequence of defective efferocytosis (Duncan et al., 2003), lupus-like autoimmunity with production of autoantibodies (Rahman et al., 2010) and defects in platelet aggregation (Chen et al., 2004). These phenotypes enabled the discovery of MERTK's involvement in efferocytosis, the phagocytic uptake of apoptotic cells mainly by macrophages and dendritic cells (Lemke, 2013), as well as regulation in the innate immune system and involvement in tissue homeostasis by promoting platelet aggregation.

Every day an estimated 130 billion cells in the human body enter apoptosis i.e. programmed cell death (Elliott and Ravichandran, 2016). During this process Phosphatidylserine (PtdSer) is exposed on the outer side of the cell membrane. MERTK on phagocytes (macrophages and dendritic cells) binds PtdSer and mediates the apoptotic cell uptake. When this function is impaired due to mutation or loss of MERTK apoptotic, cells accumulate gradually. Extensive studies on MERTK in efferocytosis have been conducted in the uptake of shed discs membrane in the retinal pigment epithelium (Shelby et al., 2015) and the phagocytic function of Sertoli cells in the testis (Lu et al., 1999).

Mechanisms of immune modulation accompany efferocytosis. In the process, phagocytic cells secrete multiple anti-inflammatory cytokines, including transforming growth factor-beta (TGFβ), interleukin (IL)-10, prostaglandin E2 (PGE2) and platelet-activating factor (PAF) (Fadok et al., 1998, Zizzo et al., 2012). Concurrently, the production of pro-inflammatory cytokines IL-1β, tumor necrosis factor-alpha (TNF-α), and IL-12 are inhibited (Huynh et al., 2002, Camenisch et al., 1999). MERTK-mediated efferocytosis promotes macrophage polarization towards M2-macrophages rather than M1-macrophages. Thus, MERTK is mainly expressed in M2-macrophages that mediate anti-inflammatory signaling, whereas pro-inflammatory M1-macrophages show lower expression levels (Pastore et al., 2019). In the tumor microenvironment, M2-macrophages exert tumor-promoting functions are frequently more abundant than M1 macrophages.

MERTK acts as a strong immune regulator in infectious diseases and prevents overshooting immune activation when Pros1 and Gas6 are in complex with AC (Pradip Sen, 2007), PtdSer or enveloped viruses (Tsou et al., 2014).

TAM receptors are also under active investigation in human vasculature diseases. MERTK activation by Pros1 has been shown to inhibit endothelial chemotaxis via induction of vascular endothelial growth factor A (VEGF-A) and tube formation migration in endothelial cells (Fraineau et al., 2012, Howangyin et al., 2016). Indirectly, $Gas^{-/-}$ results in impaired vascular integrity and $Pros1^{-/-}$ in impaired vessel formation (Burstyn-Cohen, 2017).

3.3 MERTK in Cancer

MERTK overexpression or activation has been reported in a wide range of hematological and solid cancers and is generally associated with poor prognosis (Graham et al., 2014, Hill, 2015). Target validation studies have confirmed an advantage for the tumor upon MERTK activation directly on tumor cells (Cummings et al., 2013). In breast cancer, MERTK not only mediates cell growth but also migration, angiogenesis, efferocytosis and immune suppression. Table 1 summarizes phenotypes that are positively affected by tumoral MERTK activation.

Table 1 | MERTK-associated phenotypes in solid tumors and metastasis

Cancer Entity	MERTK-driven phenotype	Reference
Astrocytoma	survival and chemoresistance	(Keating et al., 2010)
Breast	metastatic growth, migration, metastasis-free survival ,	(Tavazoie et al., 2008, Png et al., 2011) (Maimon et al., 2021)
	efferocytosis, immune suppression	(Nguyen et al., 2013, Nguyen et al., 2014) (Davra et al., 2021)
Breast, Colon, Melanoma,	T-cell immunity	(Cook et al., 2013, Lindsay et al., 2021)
Colon	inflammation	(Bosurgi et al., 2013)
Gastric	cell growth, survival	(Jun Ho Yi, 2015, Kim et al., 2017),
Glioblastoma	survival, autophagy, cell growth, chemoresistance, migration, invasion, angiogenesis	(Rogers et al., 2012, Wang et al., 2013) (Knubel Kh, 2014, Su et al., 2020)
Lung	Growth, survival, chemoresistance, immune suppression	(Linger et al., 2013, Du et al., 2021, Novitskiy et al., 2019)
Neuroblastoma	Migration, apoptosis and chemosensitivity	(Li et al., 2015)

3.3.1 MERTK in breast cancer

A study by Png et al. identify MERTK as a tumoral promoter of lung metastatic growth. After shRNA knock-down of MERTK in highly metastatic human breast cancer cells, lung metastasis progression was reduced compared to the wildtype group *in vivo* (Png et al., 2011). In lung cancer, MERTK transcriptional repression by shRNA revealed decreased colony formation *in vitro* and growth in xenograft models indicating MERTK's involvement in metastasis *in vivo*. Mechanistically, AKT, MEK1/2 and p38α were identified as downstream effectors of MERTK that activate CREB and ATF1 which control cell growth, proliferation and survival.

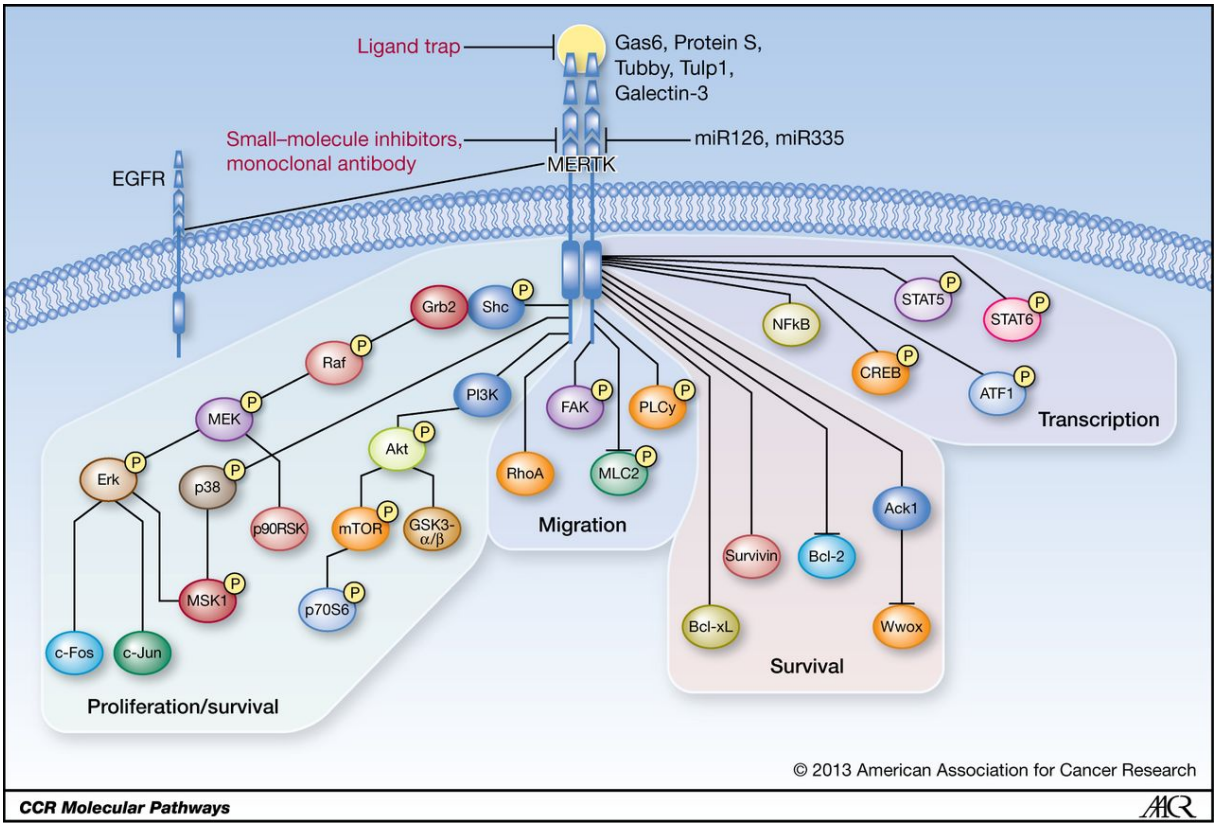

Figure 1 | Mer tyrosine kinase signaling in cancer Upon binding of MERTK by its ligands, several downstream pathways are activated that enhance cancer proliferation/survival, migration, survival and transcription. Expression of Mer is regulated by miR126 and miR335 (Tavazoie et al., 2008). Therapeutic approaches to target MERTK with ligand traps, small-molecule inhibitors and monoclonal antibodies are under investigation. Figure copied from (Cummings et al., 2013).

Other phenotypes that are linked to MERTK in human breast cancer have been found. In mammary epithelial cells (MCF10A cells) stable expression of MERTK leads to increased motility and chemoresistance through AKT activation and in human breast cancer cells (MDA-MB-231) to induce efferocytosis as a gain-of-function capacity (Nguyen et al., 2014).

With the observation of activation of TAM receptors leading to subsequent upregulation of PD-L1, it was discovered that the inhibition of TAM receptors in murine breast cancer enhances the efficacy of an anti–PD-1 mAb (Kasikara et al., 2019). This indicates a PtdSer → TAM receptor → PD-L1 inhibitory signaling axis.

3.3.2 MERTK in Metastasis

As mentioned in Figure 1, MERTK affects several downstream pathways, notably ERK, PI3K, AKT, c-Fos, which are known to be activated in EMT (Olea-Flores et al., 2019). Hence, it is of great interest to understand the regulation and activation of MERTK.

Several microRNAs (miRNA), small non-coding ribonucleic acid sequences, have been identified as suppressors of metastasis in breast cancer. The expression of these miRNAs was observed to be frequently dysregulated in metastatic breast cancer cells compared to their parental cells from primary tumors, and their expression leads to the activation of pro-metastatic pathways (Loh et al., 2019). miRNA-335 and miRNA-126 directly inhibit the expression of

MERTK (Tavazoie et al., 2008) (Png et al., 2011). Consistent with these findings, these studies showed that MERTK knock-down (MERTK-KD) in human metastatic breast cancer cells (MDA-LM2) results in reduced metastatic progression *in vivo*.

In TNBC, a novel fusion protein consisting of the signal peptide of TMEM87B, a transmembrane protein, and the transmembrane and intracellular domain of MERTK leads to phosphorylation of AKT and ERK1/2 (Shaver et al., 2016).
An unexpected function of MERTK was discovered in lung and breast cancer metastasis in which MERTK activation by myeloid cell-derived PROS1 decreased metastasis (Maimon et al., 2021).

3.3.3 Angiogenesis

Png et al. reported that MERTK-KD in tumor cells results in decreased angiogenesis *in vivo*, confirmed by reduced endothelial recruitment *in vitro.* Furthermore, sMER in human metastatic breast cancer cells was implicated in promoting endothelial migration (Png et al., 2011). The authors hypothesized that sMer acts as a decoy receptor to prevent Gas6 from binding to MERTK on endothelial cells, thereby enhancing endothelial recruitment in the process of tumor angiogenesis. Congruently, inhibition of endothelial MERTK by neutralizing antibodies results in enhanced endothelial recruitment. Furthermore, according to Fraineau et al., Pros1 is responsible for angiogenic inhibition in vascular endothelial growth factor receptor 2 (VEGFR2) via MERTK in an SHP2-dependent manner (Fraineau et al., 2012). Taken together, these findings suggest MERTK on tumor cells competes with MERTK on endothelial cells for common binding partners such as Gas6 and therefore reduces the inhibitory effect of MERTK on angiogenesis in endothelial cells.

3.3.4 Immune response in cancer

MERTK has been shown to promote tumor immune evasion, e.g., by suppressing proinflammatory cytokines (Cook et al., 2013) or polarizing tumor- associated macrophages towards an immunosuppressive state (Myers et al., 2019, Ubil et al., 2018, Crittenden et al., 2016).

One particular process in the tumor microenvironment is MERTK-mediated efferocytosis by tumor-associated M2-macrophages. Apoptotic cancer cells are engulfed by M2-macrophages that overall induce an immunosuppressive wound-healing phenotype by secreting cytokines (see section 3.2.3). Efferocytosis also prevents cancer cells to go into secondary necrosis as an alternative cell death that would expose the immune-activating intracellular compounds and tumor antigens to the immune system as the cell membrane integrity is maintained (Werfel et al., 2018).

However, it is necessary for the immune system to take up tumor-antigens specific for cancer cells to identify the tumor and to effectively develop a robust anti-tumor response (Zhou et al., 2020b). This process is usually orchestrated by professional phagocytes, so-called antigen-presenting cells (APCs) – most importantly by dendritic cells (DC). In the tumor microenvironment, APC also employ phagocytosis to take up dying cancer cells to process and present tumor-antigens to immune effector cells such as T cells.

MERTK-mediated efferocytosis by M2-macrophages works in competition with APC phagocytosis and ultimately aids the tumor in avoiding immune detection not only by creating an immunosuppressive environment but also by lowering the exposure of tumor-antigens to

APCs. Congruently, several studies have implicated efferocytosis in increasing tumor survival and metastasis in breast cancer (Mittal et al., 2018).

Cook and colleagues assessed tumor growth and metastasis in MMTV-PyVmT, a genetically induced mouse breast cancer model. After Mer –/– bone marrow transplantation into wildtype mice, tumor growth and metastasis decreased significantly. The immune cell subset of $CD11b^+$ macrophages and DC were more abundant in tumors hosted by *Mertk* $^{-/-}$ transplanted mice. These MERTK -deficient immune subsets also show increased production of proinflammatory cytokines IL-12 and IL-6 and a reduced production of anti-inflammatory IL-10. The authors concluded that the absence of MERTK specifically on $CD11b^+$ cells enables a more robust and prolonged secretion of proinflammatory cytokines compared to wildtype cells. Furthermore, a flow cytometry analysis of the tumor microenvironment showed that $CD8^+$ T lymphocytes proliferation was higher in the *Mertk* $^{-/-}$ after tumor inoculation compared to the wildtype cohort. $CD8^+$ T cells, also known as cytotoxic T cells, are generally classified as cancer-killing cells. In order to investigate the impact of $CD8^+$ T cells on mediating the effect of hematopoietic *Mer*-deletion, $CD8^+$ T lymphocytes were depleted using an anti-CD8 antibody. $CD8^+$ T cell depletion restored tumor growth in *Mertk* $^{-/-}$ mice compared to wildtype mice. A histological examination revealed that tumors in *Mertk* $^{-/-}$ mice treated with isotype control antibody grew significantly smaller and microscopically consisted mainly of fibrous tissue. In contrast, the tumors in the cohort treated with anti-CD8 antibody showed much bigger and more aggressive tumors comprised of densely packed tumor cells. This finding indicates that loss of MERTK results in a more robust anti-tumor response through increased secretion of proinflammatory cytokines, as well as activation of $CD8^+$ T lymphocytes. These effects ultimately lead to a decreased tumor growth and metastasis.

3.3.5 Therapeutic resistance

While MERTK is not an oncogenic driver, it has been implicated in supporting therapeutic resistance to chemotherapy in several tumor entities. In NSCLC, shRNA-mediated MERTK-KD enhances chemosensitivity to cisplatin and carboplatin but not doxorubicin by increased apoptosis (Linger et al., 2013). This observation suggests that MERTK contributes to an intrinsic chemoresistance in cancer cells. In neuroblastoma, MERTK inhibition by siRNA leads to increased chemosensitivity to cisplatin and vincristine (Li et al., 2015). Similar results are seen in mantle cell lymphoma treated with vincristine and doxorubicin *in vitro*. Chemotherapy in combination with UNC2250, a small molecule, show the same effect *in vivo* (Shi et al., 2018). In glioblastoma, administration of etoposid, a standard chemotherapy that causes double-strand DNA breaks, leads to robust MERTK overexpression. Furthermore, in astrocytoma, MERTK inhibition induces chemosensitivity for temozolomide, carboplatin, and vincristine and rendered one chemoresistant cell line susceptible to carboplatin. The underlying mechanism involves reduced survival signaling via ERK 1/2 and AKT (Keating et al., 2010).

Congruent with frequently detected AXL and MERTK co-expression levels in several cancer entities, MERTK levels increase as a reaction to pharmacological AXL-inhibition, indicating a functional rescue among TAM receptors (Mcdaniel et al., 2018). These findings are in line with TAM mediated PD-L1 inhibition (see section 3.3.1) as mechanisms of influencing immune response and developing therapeutic resistance.

3.3.6 Development of anti-MERTK therapies

MERTK promotes tumor progression, predominantly through its impact on cell survival (Guttridge et al., 2002) and influence on the anti-tumor immune response (see section 3.3.4). Therefore, MERTK constitutes an attractive therapeutic target.

The pharmacological inhibition of MERTK has been approached using different strategies. As mentioned above, sMER yields significant MERTK inhibition which results in decreased efferocytosis and MERTK dependent platelet aggregation and prevents thrombosis *in vivo* (Sather et al., 2007). Unfortunately, a functional ligand trap for MERTK *in vivo* has not been reported to this day.

Several small molecules show an inhibitory effect on MERTK signaling. However, the existing MERTK-binding small-molecule inhibitors that are approved by the Food and Drug Administration (FDA) are not specifically targeted at MERTK or TAM receptors but rather at multiple tyrosine kinases. Notable is Foretinib, an inhibitor against MET and VEFGR2, which shows substantial treatment effects *in vivo* in glioblastoma multiforme and might elicit its effect by binding to MERTK (Knubel Kh, 2014). In addition, small-molecule inhibitors primarily against MERTK are in ongoing clinical trials: ONO-7475 against acute leukemias and MRX-2843 against advanced metastatic solid tumors (ClinicalTrials.gov Identifier: NCT03510104, NCT03176277) (U.S. National Library of Medicine, 2020). Other specific MERTK or TAM inhibitors in preclinical development are UNC1062, UNC569, UNC1666, UNC2025, LDC1267, UNC2881, (reviewed in (Graham et al., 2014)) ONO-7475 (Ruvolo et al., 2017), ONO- 9330547 (Gilmour et al., 2016) and 6g (Suarez et al., 2013) that aim to abrogate MERTK function in either leukemia or solid tumors.

Monoclonal antibodies represent another strategy for inhibiting MERTK with potentially increased specificity and efficacy relative to small molecule inhibitors. Furthermore, not only can antibodies inhibit receptor activation, but they may also activate the immune system or deliver cytotoxic drugs to malignant cells (discussed further in chapter 3.4 and 6.5). A novel anti-MERTK neutralizing antibody exerted an anti tumor effect in combination with a PD-1 immunotherapy in breast cancer (Davra et al., 2021). Mechanistically, t-lymphocytes were recruited to the tumor sites, and the tumor microenvironment promoted more tumor immunogenicity.

A more novel approach is the inhibition of ADAM17 in order to restrict MERTK extracellular domain cleavage. An anti-ADAM17 mAb yields decreased growth, invasion and migration in triple-negative breast cancer *in vitro* (Caiazza et al., 2015). Furthermore, ADAM17 inhibition increases platinum efficacy in ovarian cancer (Hedemann et al., 2018) and *in vivo* chemosensitivity in hepatocellular carcinoma cells (Zhang et al., 2018).

3.4 Monoclonal antibodies in breast cancer

The first reported discovery of antibodies was in 1890 by the bacteriologist Shibasaburo Kitasato who described antibody activity against the diphtheria toxin (A.G.N., 1931). This led Paul Ehrlich, a German physician-scientist, to hypothesize the binding abilities of antibodies to specific antigens, a function that is utilized in therapy today to target distinct protein structures. The antigen binding site of an antibody interacts with an epitope on an antigen in a “lock and key” manner. Based on the binding affinity, molecular forces hold antibody and antigen together in an immune complex. Thus, antibody affinity is a centerpiece in defining the potential of an antibody. A monoclonal antibody (mAb) with high affinity would likely have fewer off

target effects, while low affinity would increase the chances of unwanted binding to other antigens of no therapeutic interest.

Therapeutic mAb in cancer can function in various ways that ultimately contribute to the development of an anti-tumor response. These mechanisms involve blocking binding sites of extracellular receptors and therefore hindering cell signaling by their respective ligands, the recruitment of the immune system via antibody-dependent cell-mediated cytotoxicity (ADCC) or complement-dependent cytotoxicity (CDC) and/or indirectly modulating the tumor microenvironment. In ADCC, cells are "marked" by antibodies that attract and bind to the cell surface of immune effector cells based on the antibody Fc-region that interacts with the FcγRIIIA receptor on e.g. NK cells (Clynes et al., 2000). Thus, ADCC can be increased by modifying the Fc-region or altering the glycosylation patterns of the Fc-region (Zahavi et al., 2018). CDC, on the other hand is triggered by the Fc-region activating a network of complex pathways in the complement system. Whether a mAb rather induces ADCC or CDC, depends on the type of antibody subclass.

The development of a novel mAb can be achieved with several techniques, of which the hybridoma system was employed in this study. The process undergoes several phases, which are briefly outlined as followed: Murine models are challenged with the desired antigen in order to stimulate an immune response. Next, spleen cells are extracted and immortalized to create a library of antibody-producing cells. The resulting mAbs are tested for their binding affinity and other characteristics (further details in chapter 4.3). The most promising clones are chosen for further testing in order to examine their biological effect on cell phenotypes *in vitro* e.g. impacting cell growth, differentiation or cell signaling. Next, the findings are further investigated *in vivo* which mimic a closer physiological environment to the human body. Ideally, the mechanism of action such as the influence on cell signaling or immune activation should be elucidated. If corresponding results of the preclinical phase are favorable, these may be translated further into human testing.

The epidermal growth factor receptor (EGFR) family are tyrosine kinase receptors that have first been directly linked to human solid tumors (Gschwind et al., 2004). The subsequent development of Trastuzumab (see chapter 3.1.2), a humanized recombinant monoclonal, against the HER2 receptor was the first antibody therapy against solid tumors that was approved by the FDA in 1998 and by the *European Medicines Agency* (EMA) in 2000. This paradigm shift gave rise to a new class of breast cancer drugs that could be given as monotherapy or in combination with existing chemotherapy. The antibody regimen against breast cancer was expanded by Pertuzumab, another antibody against a different HER2 epitope, and Atezolizumab, an anti-PD-L1 antibody. Pertuzumab in combination with trastuzumab and docetaxel received FDA approval in 2012 for HER2-positive metastatic breast cancer (Gianni et al., 2012). Atezolizumab in combination with nab-paclitaxel for patients with TNBC received FDA approval in 2019. Currently, an increasing number of antibodies against novel targets in breast cancer are under preclinical and clinical investigation (see https://clinicaltrials.gov)

3.5 Aim of the study

MERTK has been identified as a driver of cancer growth, metastatic behavior and prognosis in solid tumors. In recent studies, evidence of MERTK's involvement in shaping the tumor microenvironment and anti-tumor immune responses have gained more attention. These studies create the basis to further investigate the potential for manipulating its biological function in treating diseases. Furthermore, a clinically effective anti-MERTK agent has not been described

in the literature so far. To this day, there has been insufficient evidence of preclinical efficacy in targeting MERTK either on the tumor cell or in the microenvironment.

This current study investigates the role of MERTK in human breast cancer with a specific emphasis on its potential as a novel target in cancer therapy.

For this aim, the following questions were addressed:

1. What are the characteristics of a novel anti-MERTK antibody *in vitro*?
2. What is the role of MERTK in the tumor microenvironment and how does it affect cancer growth?
3. Does treating MERTK on tumor cells with an antibody elicit an anti-tumor effect *in vivo*?

4 Material and Methods

4.1 Cell culture

The MDA-MB-231 cell line that was obtained from the American Type Tissue Collection (ATCC, USA) and its highly lung metastatic derivative subline MDA-LM2 was generated in the Tavazoie Laboratory via *in vivo* selection as described previously (Tavazoie et al., 2008). Both cell lines were cultured in high-glucose DMEM medium (Gibco, USA) supplemented with 10% FBS (Sigma, USA). The mouse tumor cell lines CT26.CL25 colorectal cancer and 4T1 mammary gland cancer were obtained from ATCC and cultured in RPMI-1640 (Gibco, USA) with 10% FBS (Sigma, USA) and 1% penicillin/streptomycin.
THP-1 cells were kindly provided by Professor Paul Bieniasz from the *Rockefeller University* (New York, NY, USA) and cultured in RPMI-1640 (Gibco, USA) with 10% FBS (Sigma, USA), 1% penicillin/streptomycin (Gibco, USA), 0.4% Amphotericin B (Lonza, Switzerland) and 0.05 mM 2-Mercaptoethanol (Aldrich, USA). THP1 cells were differentiated into human macrophages by supplementing the medium with phorbol 12-myristate-13-acetate (PMA) (abcam, UK) (0.06 µg/ml) and incubating the cells for 72 h. All cell lines were cultured at 37°C and 5% CO_2 in standard tissue culture dishes (Falcon, USA). Cells were split according to the directions for each cell line by the ATCC. Confluent cells were washed 1 × with phosphate buffered saline (PBS) (Corning, USA) and detached using 1 – 3 ml of 1 × 0.25% Trypsin-EDTA (Gibco, USA). After detachment was confirmed under the microscope cells were resuspended in 10 ml of growth medium and split.

4.2 Analysis of Gene Expression levels

4.2.1 RNA isolation

RNA isolation was performed using the "Total RNA Purification Kit" (Norgen Biotek Corp., Canada). Cells from subconfluent 6-well plates (Falcon, USA) were used in triplicates. The cell culture media was aspirated, and the cell monolayer was washed with an appropriate amount of PBS. Then, PBS was carefully removed. 350 µl of "Buffer RL" were added directly to the culture plate and cells were lysed by gently tapping the culture dish and swirling buffer around the plate surface for five minutes. The cell lysate was transferred to a microcentrifuge tube. 200 µl of 100% ethanol was added, and the tube was mixed by vortexing. A column with one of the provided collection tubes was assembled. The column was filled with up to 600 µl of the lysate mix and centrifuged for 1 minute at ≥ 3,500 × g. The flowthrough was discarded and the spin column with its collection tube were reassembled. 400 µl of "Wash Solution A" to the column was applied and centrifuged for 1 minute. Washing was repeated two times and flowthroughs were discarded.
The column was spun for 2 minutes in order to thoroughly dry the resin. The collection tube was discarded. The column was placed into a fresh 1.7 ml elution tube provided by kit and 50 µl of "Elution Solution A" were added to the column. The assembly was centrifuged for 2 minutes at 200 × g, followed by 1 minute at 14,000 × g.

4.2.2 Reverse transcription polymerase chain reaction (RT-PCR)

For RT-PCR the "SuperScript III First-Strand Synthesis System" (ThermoFisher Scientific, USA) was employed. In a 0.5-ml tube the following ingredients of Table 2 were combined.

Table 2 | Preparation of RNA/primer mixture for RT-PCR

Component	Amount
1 µg of RNA	n µl

Primer (OligoDT)	1 µl
10 mM dNTP mix	1 µl
H_20 (distilled)	Add up to 10 µl total

The tube was incubated at 65°C for 5 min, then placed on ice for at least 1 min. Meanwhile, the following cDNA Synthesis Mix was prepared, each component added in the indicated order:

Table 3 | Preparation of cDNA Synthesis Mix

Component	1 reaction
10 × RT buffer	2 µl
25 mM MgCl2	4 µl
0.1 M DTT	2 µl
RNaseOUT	1 µl
SuperScript III RT (200 U/µl)	1 µl

10 µl of cDNA Synthesis Mix (see Table 3) were added to each RNA/primer mixture, mixed gently and collected by brief centrifugation. The mix was incubated at 50°C for 50 min, then at 85°C for 5 min and chilled on ice for at least 1 minute.
The tube was centrifuged briefly to collect the reaction mix. 1 µL of RNase was added and incubated for 20 min at 37°C.

4.2.3 Quantitative polymerase chain reaction (qPCR)

The "master mix" was prepared by adding 31.25 µl 2 × SYBR green mix (Applied Biosystems™, USA) to 6.25 µl H_20. 34.5 µl were transferred to an Eppendorf tube and 5.75 µl cDNA (1 µg/100 µl) was added. 35 µl/well were added to a 96-well-plate and 15 µl /well of primer mix (1mM) were added and resuspended. From the 96-well-plate 10 µl/well were transferred onto a 384-well plate in quadruplicates. The plate was sealed with "MicroAmp™ Optical Adhesive Film" (Applied Biosystems™, USA) and analyzed in a "7900HT Fast Real-Time PCR System" (Applied Biosystems™, USA). For DNA content normalization, GAPDH was used as endogenous control. The primers used are indicated in Table 4.

Table 4 | qPCR primers for Gene Expression

Gene	Forward	Reverse
MERTK	GGAGACAGGACCAAAGC	GGGCAATATCCACCATGAAC
GAPDH	AGCCACATCGCTCAGACAC	GCCCAATACGACCAAATCC

4.2.4 Data Analysis

Comparative Quantification was calculated with the following equations:

$Ct_{GOI} - Ct_{norm} = \Delta Ct$
$\Delta Ct_{sample} - \Delta Ct_{calibrator} = \Delta\Delta Ct$
Cycles to Threshold (Ct), Gene of interest (GOI), normalization (norm),

4.3 Anti-MERTK antibody development

The mouse anti-MERTK antibody, clone M6M3, was previously developed by the Tavazoie laboratory at the *Rockefeller University* (USA) (Patent # EP3237450). Mice were vaccinated with recombinant Human MERTK Fc Chimera Protein (R&D Systems, USA). Murine spleen cells were extracted and fused with human myeloma cells to produce hybridoma clones. The antibody clone M6 was picked for its ability to suppress endothelial recruitment phenotypes *in*

vitro and primary tumor growth *in vivo*. For this thesis, M6M3, a subclone of M6, was used. Antibody protein was synthesized according to standard hybridoma techniques by BioXCell (West Lebanon, USA).

4.4 Antibody affinity assay

This protocol is largely an adjustment of the protocol by Martineau (Martineau, 2010), which refers to the original approach by Friguet et al. (Friguet et al., 1985) with the optimization for measuring K_D for bivalent antibodies by Stevens et al. (Stevens, 1987).

4.4.1 Establishing coating antigen-concentration by ELISA

Two Flat-bottom ELISA plates (Nunc Maxisorp, Thermo Fisher Scientific, USA) were coated with either 50 nM solution of hMer-Fc (R&D Systems, USA), hMer-DDDK (Sino Biologicals, China) or mMer-Fc (Sino Biologicals, China) prepared in PBS (Corning, USA) and serially diluted 1:2. After overnight incubation at 4°C, the plates were washed 3 times with 200µl PBST/well (PBS with 0.1% (v/v) Tween-20 (Promega, USA). Then, 150 µl/well of PBSM (PBS with 3% (w/v) non-fat dried milk (Great Value ™, USA) were added and incubate for 2 h at room temperature.

Plate 1
Plate 1 was then washed 3 times with 200µl PBST/well. A series of 2-step dilutions of M6M3 antibody were prepared at the indicated concentration in PBS. 100 µl of each dilution, in triplicate, were added to the plate and incubated for 1h. Afterwards, the M6M3 antibody solution was pooled. Excess antibody was removed by washing 3 times using 200µl PBST/well.

Plate 2
The M6M3 antibody solution from plate 1 was added to plate 2 in the same manner as described above and incubated at RT for 1 hour.

Both plates were then incubated with 100 µl/well of AP-conjugated anti-mouse antibody (Sigma, USA, A3562) diluted 1/3,000 at RT for 1 hour. Plates were washed with PBST and 100 µl/well of PNPP (Sigma, USA) were added and incubated for 90 min at RT. Finally, plates were measured in an ELISA reader (Infinite F200, Tecan, Switzerland) at 405 nm

4.4.2 Measuring unbound antibody as a function of antigen concentration

A flat-bottom ELISA plate was coated with 100 µl of a 0.1 µg/ml solution of either hMer-Fc at 0.01µg/ml or hMer-DDDK at 0.05µg/ml prepared in PBS. 150 µl/well of PBSM were added and incubated for 2 h at RT for saturation. Serial 1:2 dilutions of the antigens (also used in section 4.4.1) in PBS were prepared, in a final volume of 150 µl and repeated 9 times. An antibody dilution at twice the maximal concentration determined in ELISAs in section 4.4.1 were prepared. The minimum volume should be of 150 µl * (number of antigen dilutions +1). Then, 150 µl of antibody were added to each antigen dilution and incubated for 1 h at RT. Lastly, the plate was measured in an ELISA reader (Infinite F200, Tecan, Switzerland) at 405 nm

A flat-bottom ELISA plate was coated with 100 µl of a 0.1 µg/ml solution of either hMer-Fc at 0.01µg/ml or hMer-DDDK at 0.05µg/ml prepared in PBS.
- 150 µl of PBSM were added to each well and incubated for at least 2 h at RT. - During the saturation, serial 1:2 dilutions of the antigen in PBS were prepared, in a final volume of 150 µl and repeated 9 times.

An antibody dilution at twice the maximal concentration determined in ELISAs in section 2.10.1 were prepared. The minimum volume should be of 150 µl * (number of antigen dilutions +1).
150 µl of antibody were added to each antigen dilution and incubated for 1 h at RT.
The plate was measured in an ELISA reader (Infinite F200, Tecan, Switzerland) at 405 nm

The K_D-value was calculated with the following equation using Graphpad Prism:

$$A = (A_{max} - A_0) \times \left[\frac{\sqrt[2]{(X - Ab_{conc} + K_d)^2 + 4 * K_d * Ab_{conc}} - (X - Ab_{conc} + K_d)}{2 * Ab_{conc}}\right] \times \left[\frac{(X + Ab_{conc} + K_d) - \sqrt[2]{((X + Ab_{conc} + K_d)^2 - 4 * X * Ab_{conc})}}{(2 * Ab_{conc}) + 1}\right]^{(-1)+Ao}$$

A is the absorbance, A_{max} and A_0 are, respectively, the maximal and minimal absorbance signal obtained by ELISA (when x = 0 and x = ∞), K_D is the dissociation constant, Ab_{conc} is the total concentration of M6M3, X is the number of binding sites per antigen.

4.5 Western Blot

Cells were washed with ice-cold PBS, scraped off from cell culture dishes using a cell scraper (Falcon, USA) and lysed in 0.1 – 1 ml of ice-cold RIPA buffer (G Biosciences, USA) supplemented with protease inhibitors (Roche, Switzerland) and phosphatase inhibitor "PhosSTOP" (Roche, Switzerland). The protein concentration was measured using a "Pierce™ BCA Protein Assay Kit" (ThermoFisher Scientific, USA). 20 – 40 µg of protein lysate per sample mixed with 1 × LDS buffer (Novex) and 1 × reducing agent (Invitrogen) were boiled at 95°C for 5 minutes. Proteins were separated on a Bis-Tris 4-12% SDS-PAGE (Invitrogen), and transferred wet to a 0.45µm PVDF membrane blot (Immobilon-P) in 1 × Transfer Buffer (Thermo Fisher Scientific, USA) containing 20% methanol at 80V for 2 h at 4˚C. For protein size identification Precision Plus Protein(tm) Dual Color Standards (Bio-Rad) were used. Then, the blot was blocked in TBST containing 0.1% Tween 20 (Promega, USA) and 5% Bovine serum albumin (BSA, Sigma, USA). Afterwards, the membrane was stained with primary antibodies at 4°C over night at the concentrations indicated in table Table 5. On the next day, the membrane was washed 3 times with TBST and stained with secondary antibody at room temperature for 1h. Primary antibodies were diluted in TBST containing 3% BSA and 0.02% Na-azide (Ricca Chemical Company, USA) and secondary antibodies were diluted in TBST. The following antibodies were used for protein detection:

Table 5 | Primary and secondary antibodies used in Western Blot analysis

	Antibody	Manufacturer	Dilution
Primary antibody	anti-Axl (C89E7) rabbit mAb, #8661	Cell signaling, USA	1 : 1000
	anti-MERTK (human) rabbit mAb, Y323	R&D Systems, USA	1 : 1000
	anti-GAPDH mouse mAb, (GT239)	GeneTex, USA	1 : 1000
Secondary antibody	HRP-Goat Anti-Rabbit IgG (H+L) DS Grd	life technologies, USA	1 : 3000
	ECL Anti-mouse IgG, HRP linked whole antibody (from sheep)	GE Healthcare UK limit, UK	1 : 10 000

Next, the blot was washed three times with TBST for 5 minutes and incubated using a PIERCE ECL Western blotting substrate kit (Thermo Fisher Scientific, USA) for one minute. The Western Blot film was developed using in an SRX 101A Film Processors (Konica, Japan).

4.6 Fluorescence-activated flow cytometry (FACS)

At least 100 000 cells were lifted by scraping from standard tissue culture plates using cell scrapers (Falcon, USA), washed with FACS buffer consisting of PBS (Corning, USA), 2% FBS (Sigma, USA), 10mM EDTA , 0.1% Na-azide (Riccardo Chemical Company) and 25mM HEPES (Gibco, USA) and stained for 10 minutes with an Fc-blocking TruStain fcX™ anti-human CD16/32 antibody (BioLegend) diluted at 1:200 in FC buffer. Cells were stained for 20 minutes directly with PE conjugated MERTK antibody (clone:590H11G1E3, BioLegend) at 1:900 final concentration. For assessing the total MERTK levels cells were permeabilized using a Fixation/Permeabilization Solution Kit (BD Biosciences) according to the manufacturer's directions and then stained as described. PE conjugated IgG1κ (clone: MOPC21, BioLegend, USA) was used as an isotype control. Samples were processed using a BD LSRFortessa™ (BD Biosciences, USA) and analyzed using *FlowJo, LLC* (Becton, Dickinson & Company, USA).

4.7 Cancer cell proliferation assay

2.5×10^4 cells were seeded in quadruplicates onto 6-well-plates. 12 hours later the medium was exchanged with complete medium supplemented with either 1µg/ml IgGκ MOPC21 (IgG) (BioXCell, USA) or anti-MERTK antibody M6M3. The medium was changed after every 2 days supplemented with 10µg/ml antibody. Viable cells were counted using 0.4% Trypan Blue solution (ThermoFisher Scientific, USA) at 5 days after seeding.

For proliferation assays under starvation conditions, 3×10^5 cells were seeded in quadruplicates onto 6-well-plates. The next day, the cells were washed with PBS (Corning, USA) and cultured in DMEM (Gibco, USA) containing 0.02% FBS (Sigma, USA) supplemented with either 10µg/ml IgG control or anti-MERTK antibody M6M3. 72 h later, viable cells were counted using 0.4% Trypan Blue solution (ThermoFisher Scientific, USA).

4.8 Colony formation assay

In order to assess colony formation assay this method was adapted from Franken et al. (Franken et al., 2006). Cells were seeded in three biological replicates onto a 6-well-plate and cultured in complete growth medium overnight. The next day, medium was exchanged with complete growth medium supplemented with either with IgGκ MOPC21 (BioXCell, USA) as either an Immunoglobulin G (IgG) isotype control or anti-MERTK antibody M6M3 at a concentration of 1µg/ml. 72 h later confluent cells were detached using 0.25% Trypsin-EDTA (Gibco, USA), counted using 0.4% Trypan Blue solution and from each biological replicate 1000 cells/well were seeded in triplicates onto 6-well-plates. Cells were cultured in complete growth medium for 10 days. Every 5 days, medium was exchanged for fresh complete growth medium without antibody. On day 10, medium was removed, and cells were washed carefully with PBS. Each well was stained with 2 – 3 ml crystal violet staining solution (glutaraldehyde 6.0% (volume/volume) (Spectrum Chemical, USA), crystal violet 0.5% (weight/volume) (Sigma, USA) in ddH_2O for at least 30 minutes. Wells were submerged in tap water in order to remove excess staining solution. Afterwards, the samples were dried at room temperature. Pictures were taken in a FluorChemQ system using trans white light and each well was analyzed for colony

count and stained area covered using a customized pipeline in *CellProfiler* version 2.2.1 (Vokes and Carpenter, 2008)

4.9 Animal Studies

All animal experiments were conducted in agreement with a protocol approved by the Institutional Animal Care and Use Committee (IACUC) at the *Rockefeller University*. NOD-*scid*, NOD-*scid* IL2Rgamma^{null} (NSG), C57BL/6, BALB/cJ and the B6;129-Mertkt^{m1Grl}/J, a *Mertk* $^{-/-}$ mouse strain, were obtained from the *Jackson Laboratory*. *Mertk* $^{-/-}$ mice were backcrossed onto C57BL/6J and BALB/c backgrounds at least five times for *in vivo* experiments and a MERTK heterozygous colony served as breeders for experimental mice.

4.10 Genotyping

4.10.1 DNA isolation from ear biopsy

Ear biopsies were obtained from mice using an ear punch pincher (Braintree Scientific Inc. EP-SA 7000). Each sample was digested in 197.5 µl DNA direct tail lysis buffer (Viagen, USA) with 2.5µl proteinase K (20mg/ml, Roche, Switzerland) at 55°C for 5 h, 85°C for 15 min in a PCR cycler (C1000 Touch™ Thermal Cycler, Bio-Rad, USA) and stored at 4°C for up to 6 months.

4.10.2 Polymerase chain reaction (PCR)

Each sample was mixed with the following reagents and then loaded onto 96-well PCR plates:

Table 6 | PCR reaction mixture from genotyping sample

1.	JumpStart™ REDTaq® ReadyMix™ (Sigma-Aldrich, USA)	5µl
2.	Molecular Biology Grade Water (Corning, USA)	2.5µl
3.	PCR primer mix (forward & backward) 20µM	0.5µl
4.	Genotyping sample	1µl

The PCR primers are indicated in Table 7

Table 7 | PCR primers for Gene Expression

Gene	Forward	Reverse (common)
Mertk-wildtype	TGCCATTATACCTGGCTTTCA	CATCTGGGTTCCAAAGGCTA
Mertk-mutant	ATCAGCAGCCTCTGTTCCAC	

PCR samples underwent conditions indicated in Table 8 in a PCR cycler.

Table 8 | PCR reaction conditions for Gene Expression

Step	Temperature	Time	function
1.	94°C	3 min	denaturation
2. (repeated 35 times)	94°C	30 sec	
	63°C	40 sec	annealing
	72°C	1 min	elongation
3.	72°C	2 min	
4.	10°C	hold	

Expected DNA band sizes for MERTK-wt is 235 basepairs (bp) and for MERTK-mutant is 250 bp. *Mertk* $^{-/-}$ mice would only show the mutant band whereas heterozygous mice would show both bands in a gel electrophoresis

4.10.3 Gel electrophoresis

The DNA electrophoresis was done on a 3% agarose gel that was mixed together with Agarose powder (Lonza, Switzerland) dissolved in 1 × TAE-buffer (Bio-Rad, USA) by microwaving. For DNA visualization ethidium bromide (Teknova, USA) was added at 1µl/16ml of heated agarose gel mix resulting in a concentration of 625ng/ml. The gel was poured into an "Owl™ EasyCast™ B2 Mini Gel electrophoresis system" (ThermoFisher Scientific, USA). PCR and a 1 Kb Plus DNA Ladder (ThermoFisher Scientific, USA) were loaded onto the solidified gel and the gel ran at 90V for 90 min. Afterwards the gel was imaged under UV light in a FluorChem Q system (CellBiosciences, USA).

4.11 Primary Tumor Growth assay

For the subcutaneous tumor growth assay, CT26 colon cancer cells at 2 × the desired cell concentration (as indicated in the results section) were resuspended in PBS and mixed 1:1 with matrigel (Corning, USA) and injected subcutaneously into the right flank of 6-8 weeks old, sex-matched BALB/c MERTK wildtype vs. *Mertk* $^{-/-}$ mice.
For the mammary gland tumor growth assay, 4T1 cancer cells were prepared identically and injected directly into the 4th mammary fat pad of 6-8 weeks old, female, BALB/c MERTK wildtype vs. *Mertk* $^{-/-}$ mice.
For the xenograft model, MDA-MB-231 human breast cancer cells were injected into 6-8 weeks old, female, NOD-SCID or NSG mice as indicated. Once tumors reached a size of 50 mm^3, mice were randomized and treated with 200µg of IgGκ MOPC21 (BioXCell, USA) isotype control antibody or anti-MERTK antibody M6M3 by intraperitoneal injection three times a week.
All tumors were measured every 2-3 days after tumors were palpable. Tumor dimensions were measured using a *Traceable* digital caliper (Fisher Fisher Scientific, USA), and tumor volume was calculated as (small diameter)^2 × (large diameter)/2. When tumors reached a volume >1500mm^3, animals were sacrificed.

4.12 Tail vein assay of lung metastasis

For metastasis assays, previously described MDA-LM2 cells expressing a Luciferase reporter were used (Png et al., 2011, Ponomarev et al., 2004). Cells were detached and resuspended in complete growth medium and strained through a 70 µm filter. Cells were counted, spun down and resuspended in PBS and adjusted to 1 × 10^6 cells/ml. Cells were then strained through a 40 µm filter and counted again. The cell number was adjusted to 5 × 10^5 cells/ml. for intermediate storage, the cells were placed on ice. Mice were pre-warmed at 38ºC and restrained in a Tailveiner (AgnTho's, Sweden). A 1 ml syringe (28 1/2 g insulin injection needle) was filled with 100µl well-resuspended single cell suspension and laid horizontally on ice. The distal third part of the mouse tail was cleaned with ethanol and the lateral vein was localized. 100µl of cell suspension were injected intravenously.
For metastatic imaging of the lungs, 100 µl of D-luciferin potassium salt (Sigma-Aldrich, USA) dissolved in PBS at a final concentration of 16.67µg/ml were injected retro-orbitally. Then, mice were placed in an IVIS Lumina LT (PerkinElmer, USA) and pictures were taken after a 30 second or 1 minute exposure. Results were normalized to the signal on day 0 right after the injection and analyzed in *Living Image* (PerkinElmer, USA), a data processing software.

4.13 Immunofluorescent staining

Mouse lungs were resected at the termination of a tumor growth study and fixed in 4 % PFA (Alfa Aesar) over night and stored in 70% ethanol for long term storage. Then lungs were embedded in paraffin and sectioned by *Histoserv Inc.* (Germantown, MD, USA) at 5µM thickness. For immunofluorescent staining the lung sections were treated the following way:

Table 9 | Immunofluorescent staining of histopathological tissue sections

Deparaffinazation	Dewax in 100% Xylenes (Fisher Chemical, USA) 2 × 3 minutes Xylenes 1:1 with 100% ethanol (Decon Labs, USA) for 3 min 100% ethanol: 2 × 3 min 95% ethanol: 3 min 70 % ethanol: 3 min 50 % ethanol: 3 min Running cold tap water to rinse
Antigen retrieval	1 × 95-100˚C Citrate (Sigma, USA) pH 6 for 20 min cold PBS for 5 minutes
Blocking	PBS with 5% goat serum (Sigma-Aldrich, USA) for 60 min
Primary antibody staining	Antibody diluted in PBS with 5% goat serum at 4˚C over night: • Cleaved caspase-3 (clone V.7C7, abcam, UK) 1:400 dilution • Endomucin (polyclonal, abcam, UK) 1:200 dilution
Secondary antibody staining	Diluted in PBS with 5% goat serum at room temperature for 45 min: • Alexa Fluor 488 goat anti-rabbit (abcam, UK), 1:200 dilution • Alexa Fluor 555 goat anti-rat IgG (abcam, UK), 1:200 dilution
	Wash 3 times with PBS • as part of the second wash incubate with DAPI (Roche, Switzerland) 1µg/ml for 5min
Mounting	Mount using one drop of Prolong Gold (Thermo Fisher Scientific, USA) and cover with a 24mm cover glass (Thermo Fisher Scientific, USA). Let slide dry at room temperature

Stained slides were imaged by an inverted TCS SP8 laser scanning confocal microscope (DMI 6000, Leica, Germany) at the corresponding wavelength of the secondary antibodies. The obtained pictures were analyzed using a custom pipeline in *Cellprofiler* version 2.2.1.

4.14 Statistical Analysis

Averages were compared using Student's t-tests as indicated in the figures and visualized with Prism software version 6 (GraphPad Software).

5 Results

5.1 Anti-MERTK mouse monoclonal antibody M6M3 binds to human MERTK.

The effect of an anti-tumor therapy that is elicited by an antibody depends in part on the binding affinity of the antibody to its antigen (Stephen I. Rudnick, 2009). The anti-human-MERTK mouse monoclonal antibody, M6M3, was previously developed in the *Tavazoie Laboratory* and selecting for this specific antibody clone through *in vitro* endothelial recruitment assays and preliminary primary tumor growth studies *in vivo*. In order to assess whether M6M3 does bind to its antigen with high affinity, the K_D value of antibody binding was determined by an ELISA affinity assay. M6M3 exhibited a low or respective non-detectable binding affinity to murine MERTK (see Figure 3) but showed a high binding affinity to human MERTK with an average $K_D = 0.94$ at antigen concentrations in the nM range (see Figure 2). These results are consistent with previous binding affinity studies by the Tavazoie Laboratory in which a Plasmon resonance system was employed (data not shown).

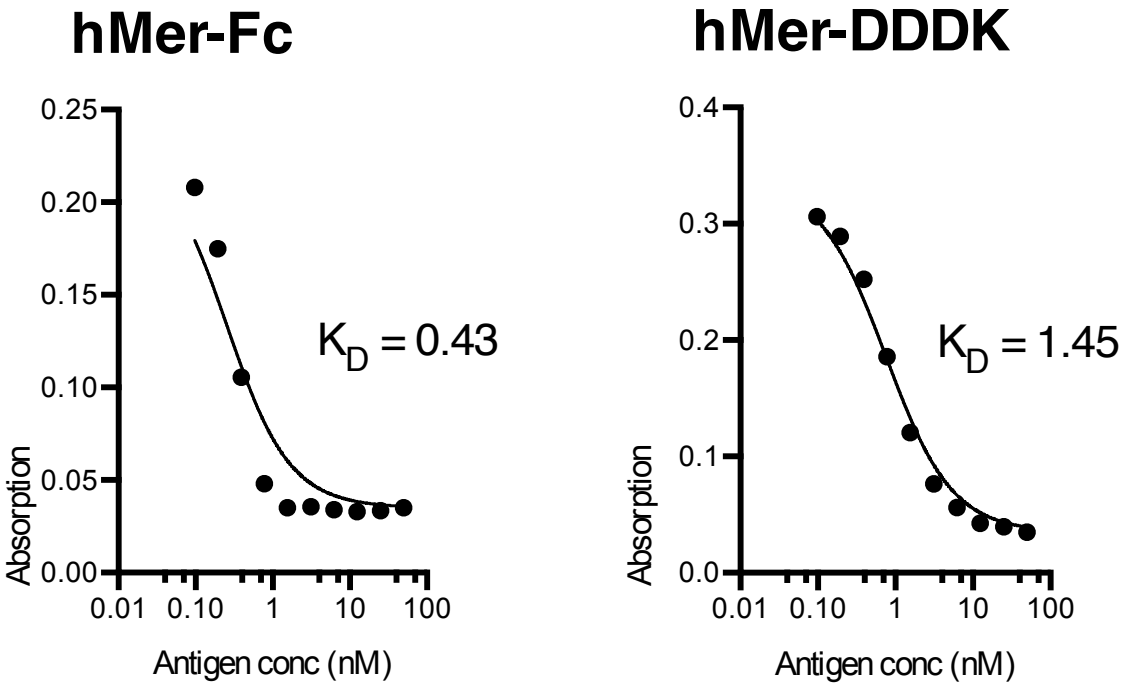

Figure 2 | M6M3 binds to human MERTK with high affinity.
An ELISA affinity assay coated with human MERTK bound to the human antibody Fc-part (hMer-Fc), or a DDDK-tag (hMer-DDDK) demonstrated high binding affinity of M6M3 to human MERTK protein. K_D values are indicated in figure (unit in nM). Analysis was performed by applying a non-linear regression curve.

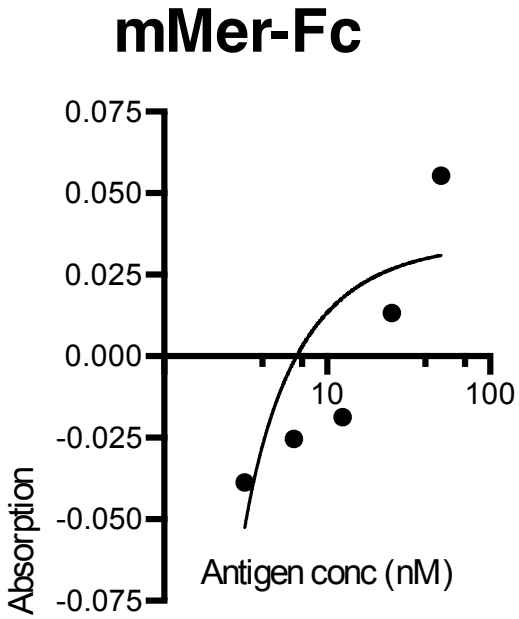

Figure 3 | M6M3 has no binding affinity to murine MERTK.
An ELISA affinity assay coated with murine MERTK bound to the human antibody Fc-part (mMer-Fc) demonstrated only unspecific binding and thus, no substantial binding affinity of M6M3 to murine MERTK protein . Analysis was performed by applying a non-linear regression curve.

5.2 MERTK gene expression levels in human breast cancer

MERTK was previously found to be overexpressed by highly metastatic breast cancer sublines, at least in part as a result of post-transcriptional regulation (Tavazoie et al., 2008). To determine whether genomic copy number alterations contribute to MERTK overexpression, the breast cancer cell line MDA-MD-231 and its *in vivo* selected derivative subline that shows enhanced metastatic colonization of the lungs, MDA-LM2, were studied for genomic MERTK copy number status. The genomic copy number of MERTK was found to be increased in MDA-LM2 over the parental MDA-MD-231, consistent with the notion of copy number gain contributing to MERTK overexpression in highly metastatic breast cancer (Figure 4).

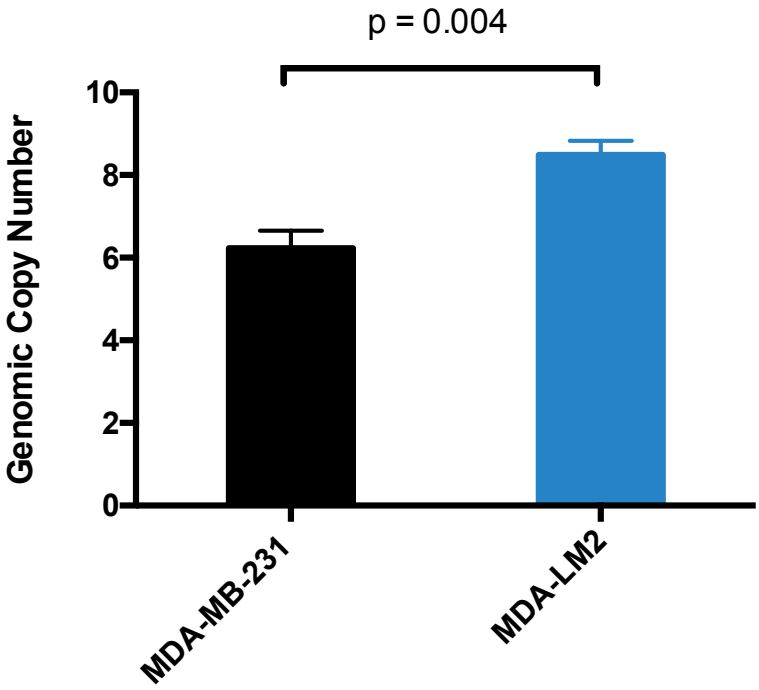

Figure 4 | Genomic copy number analysis reveals higher MERTK copy number in the metastatic subline MDA-LM2 compared to its parental human breast cancer cell line MDA-MB-231 Genomic qPCR was performed on DNA from the MDA-MB-231 primary malignant cancer cell line and its highly lung metastatic subline MDA-LM2. n > 3; Data are represented as mean ± SEM, p-value obtained using a one-sided Student's t-test.

5.3 Treatment of breast cancer cells with M6M3 leads to MERTK receptor internalization and degradation *in vitro*

In order to characterize the effect of M6M3 on cancer cells, MDA-MB-231 human breast cancer cells and its highly lung metastatic derivative subline MDA-LM2 were treated *in vitro* with either M6M3 or IgG control Ab and assessed for MERTK protein levels via Western Blot. As shown in Figure 5, in MDA-MB-231 cells MERTK levels were reduced by a substantial amount upon treatment with M6M3 in a dose-dependent manner. The abundance of the closely related TAM receptor AXL remained unchanged. MERTK levels decreased similarly in the highly metastatic MDA-LM2 cells. Interestingly, however, we noticed increased abundance of AXL levels upon M6M3 treatment in the MDA-LM2 cell line. Cells were also analyzed using fluorescence activated flow cytometry, allowing for the assessment of both surface and total MERTK levels. MDA-MB-231 cultures were treated with 10 µg/ml M6M3 or 10 µg/ml IgG for 24h and then stained either for surface or total cell MERTK levels with PE-conjugated fluorescent antibodies. Congruent to the previous finding, MERTK levels were reduced on the cell surface by ~ 64% ($p \leq 0.0001$) and in the total cell by ~ 39% ($p \leq 0.00001$). Furthermore, MERTK of M6M3-treated cells were higher on the total than surface level by ~ 38% ($p \leq 0.000005$).

(A)

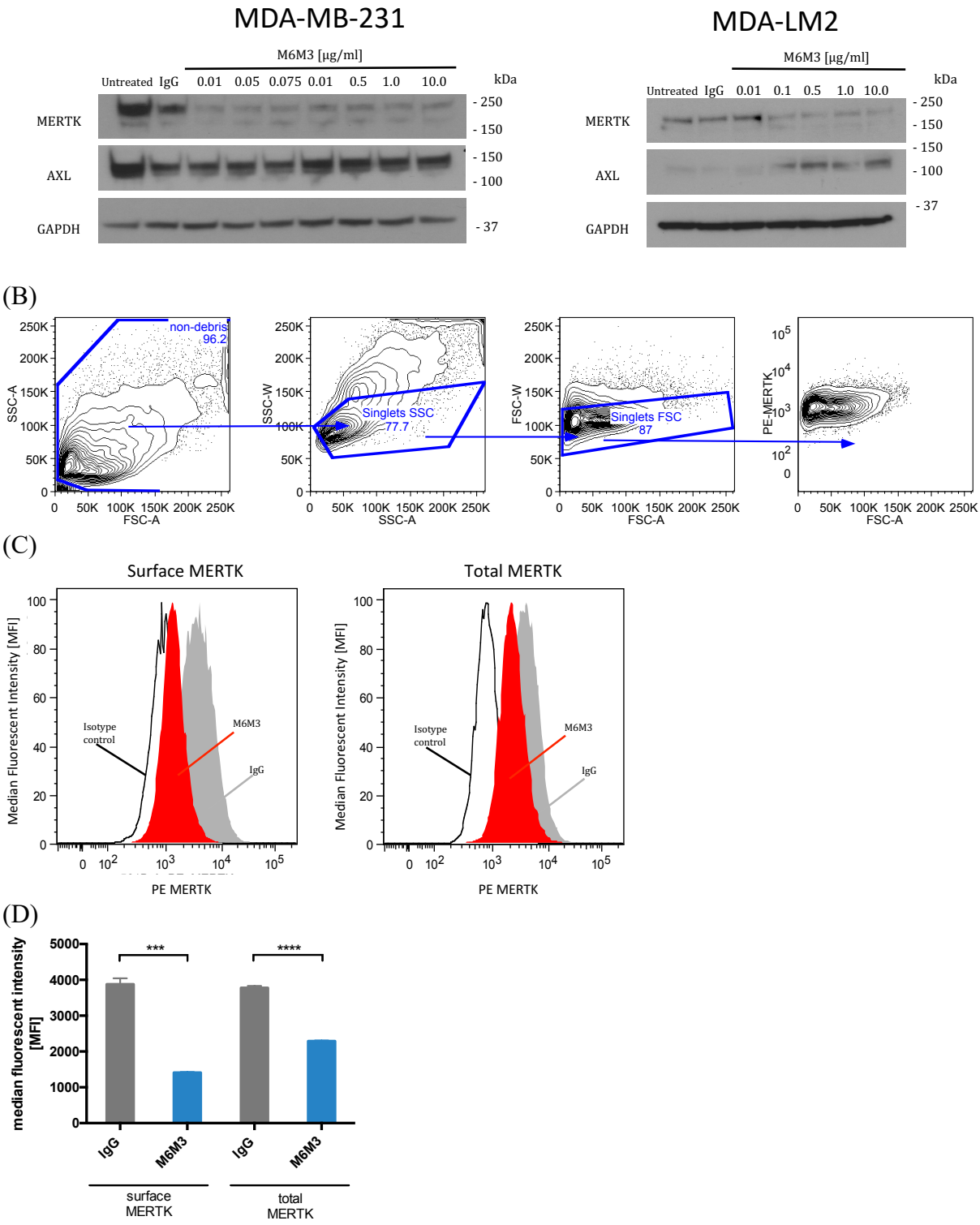

Figure 5 | M6M3 leads to reduced total cellular and surface expression of MERTK
(A) MDA-MB-231 and its highly metastatic clone MDA-LM2 were cultured in the presence of M6M3 or isotype control murine IgG control for 24h (concentrations and incubation time indicated in annotations). GAPDH was used as a loading control. Protein size indicated in KDa (B) Gating hierarchy of cells that were analyzed using fluorescent-activated flow cytometry (C) MDA-MB-231 cultures were treated with 10 µg/ml M6M3 or 10 µg/ml mIgG for 24h and then either stained for surface (left panel) or total cellular expression (right panel) of MERTK and analyzed by flow cytometry n = 3. (D) Bar representation of MFI measurements. All data are

represented as mean ± SEM, p-value obtained using a two-sided Student's t-test (*** p≤0.001, **** p≤0.0001).

5.4 M6M3 does not affect cancer cell proliferation *in vitro*

We next assessed the impact of the M6M3 antibody on cancer proliferation *in vitro*. Both MDA-MB-231 and MDA-LM2 cells that were cultured in proliferation assays supplemented with M6M3 (10µl/ml) did not exhibit a significant change in proliferation rate over a period of five days (see Figure 6). Equally, the number of dead/apoptotic cells remained unchanged (data not shown). Next, in order to increase the selection pressure on proliferative cells, cells were cultured in a nutrient low starvation assays supplemented with M6M3 at the same concentration. Similarly to the proliferation assay in full medium, the proliferation rate under starvation conditions did not exhibit a significant difference between treatment with M6M3 antibody and antibody isotype control.

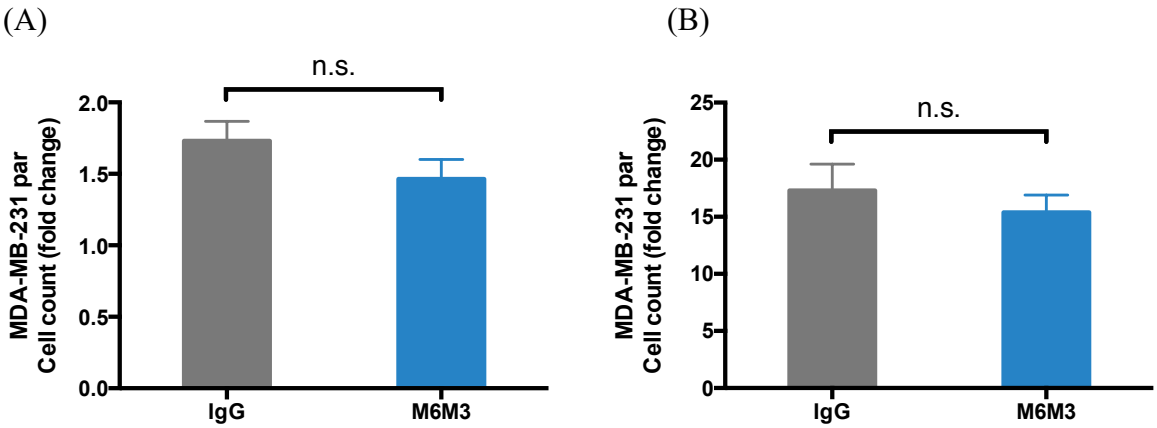

Figure 6 | M6M3 treatment does not lead to inhibition in proliferation in full and starvation mediumMDA-MB-231 were seeded in concentrations of (A) 2.5×10^4 cells under full medium (10% FBS) and (B) 3×10^5 cells under starvation medium (0.02% FBS). Either M6M3 or isotype control murine immunoglobulin (IgG) control (at 10µl/1ml) were added to the medium and cells were cultured for 5 days. Viable cells (trypan blue negative) were counted and normalized to the seeding number. All data are represented as mean ± SEM, p-value obtained using a two-sided Student's t-test(n.s. = not significant).

5.5 M6M3 inhibits cancer colony formation

In light of the drastically reduced abundance of MERTK upon treatment with M6M3 as determined by Western Blot analysis, we next assessed the effects of M6M3 on the colony formation ability of cancer cells. In the process of forming distant sites tumor cells require to have a strong repopulation ability. This assay studied *in vitro* repopulation of cells after an initial treatment with M6M3 for 72 h. After 10 days, colonies that formed from single cells were stained and counted. MDA-MB-231 cells showed a reduction of ~ 20% ($p = 0.00096$) and MDA-LM2 a reduction of ~ 11% ($p = 0.023$) after treatment compared to the control group (see Figure 7). Since proliferation and apoptosis phenotypes were unchanged by M6M3 in previous experiments a certain selection for slow growing cells was seen as an unlikely possibility. Thus, these results support the notion that MERTK may be involved in the process of repopulation.
(A)

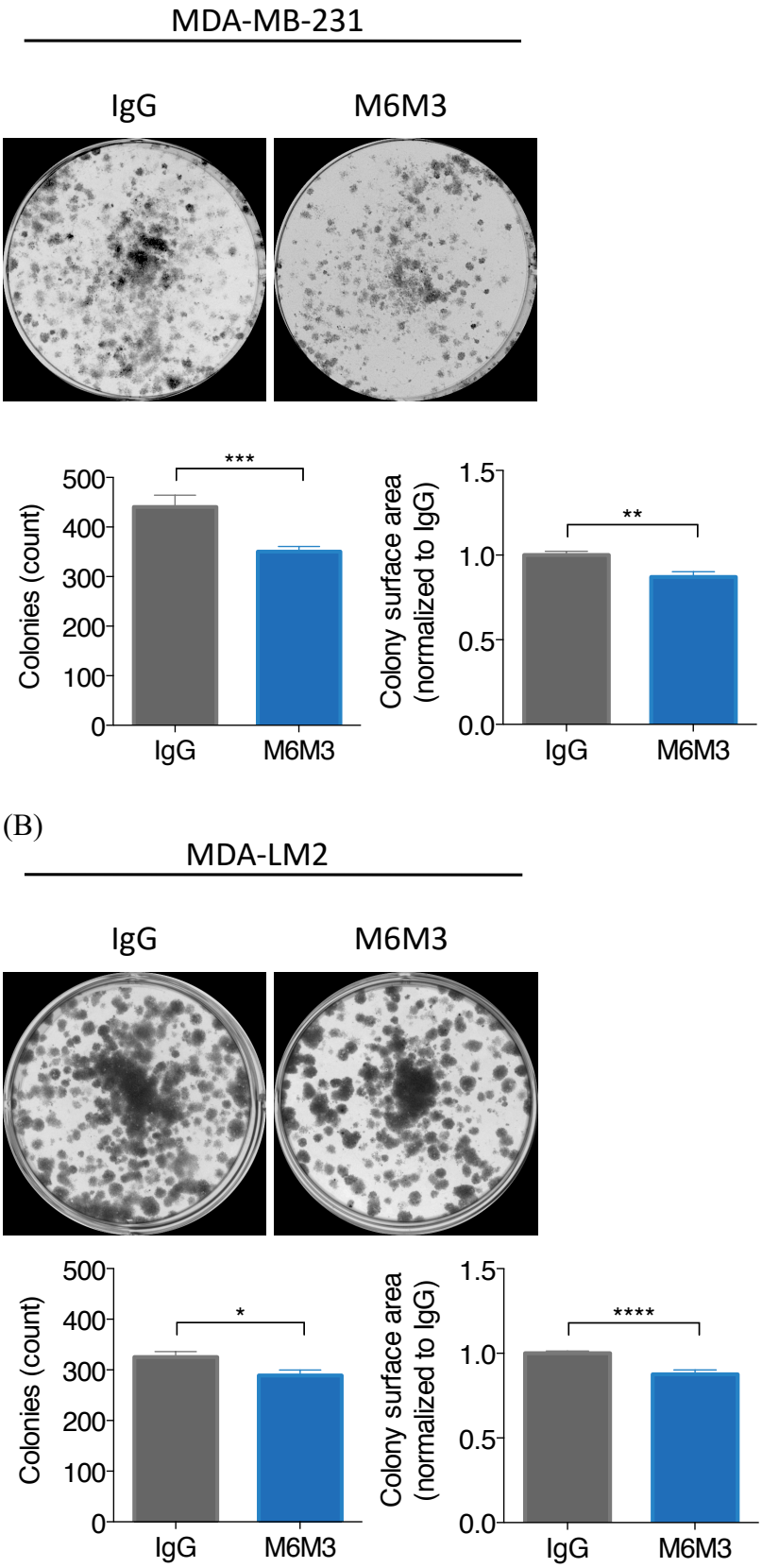

Figure 7 | M6M3 leads to reduced colony formation in human breast cancer cells
(A) MDA-MB-231 or (B) MDA-LM2 were treated with M6M3 1µg/ml vs IgG control for 72h, then dissociated, stained with trypane blue and viable cells were counted. 1000 cells/well were re-plated in complete media without antibody. Colonies were stained with crystal violet and quantified after 10 days. Quantified colonies (n) and area covered shown in histogram. n = 9.

All data are represented as mean ± SEM, p-value obtained using a two-sided Student's t-test (* p≤0.05, **p≤0.01, ***p≤0.001, **** p<0.0001).

5.6 Impact of host MERTK knock-out on tumor progression *in vivo*

Previous studies have suggested an impact of MERTK expressed by the microenvironment to impact *in vivo* tumor progression phenotypes, such as endothelial recruitment and tumor-immune interactions (Cook and Swayne, 2007, Png et al., 2011). In order to assess the impact of MERTK expressed by the microenvironment we used *Mertk*-knockout mice, which allowed us to study the role of microenvironmental MERTK on tumor progression in immune-competent hosts. We assessed two syngeneic tumor models in wildtype versus *Mertk* $^{-/-}$ mice: CT26 colorectal carcinoma and 4T1 mammary carcinoma. CT26 tumors exhibited a significant growth reduction of ~ 40% (p = 0.03) in the *Mertk* $^{-/-}$ compared to the wildtype cohort in data from two pooled *in vivo* experiments (see Figure 8). On the other hand, 4T1 tumors showed comparable growth rates in the *Mertk* $^{-/-}$ cohort compared to wildtype in two independent experiments with different cell concentrations (see Figure 8). These findings suggest that host-derived MERTK promotes tumor progression in a cancer-specific fashion.

CT26:

(A)

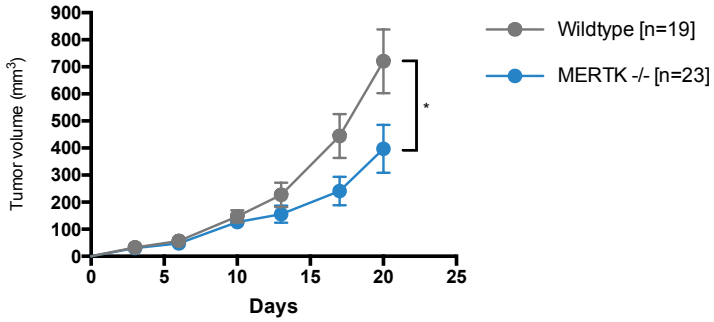

4T1:

(B)

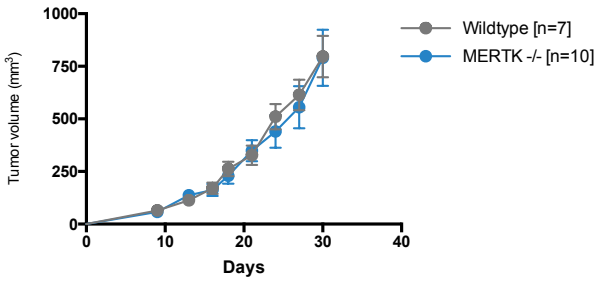

(C)

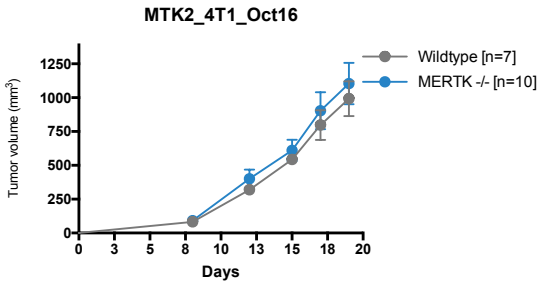

Figure 8 | The impact of stromal deletion of MERTK on tumor progression is tumor model-dependent

(A) Tumor growth of 2 × 10^5 CT26 colon cancer cells injected subcutaneously into BALB/c mice (data from two independent experiments). p > 0.05 (B) 2 × 10^3 4T1 breast cancer cells and (C) 1 × 10^4 4T1 cells injected into the 4th mammary fat pad of BALB/c mice. When tumors were palpable volumes were measured every 3 – 4 days. Sample sizes indicated in figure. All data are represented as mean ± SEM, p-value obtained using a two-sided Student's t-test (* p≤0.05).

5.7 Microenvironmental MERTK-expression does not affect microvascular vessel density or apoptotic cell abundance in tumors

Next, tumors of *Mertk* $^{-/-}$ or wildtype mice were resected upon termination of the experiments and cut into 5 µm sections and stained either with Hematoxylin an Eosin or with immunofluorescent antibodies to assess microvascular vessel density and quantity of apoptotic cell. As seen in Figure 9, there was no significant difference in microvascular vessel density in either CT26 or 4T1 tumor models between the wildtype and *Mertk*-knockout cohorts. When counting apoptotic cells that were positive for cleaved-caspase3 there was a trend towards more apoptotic cells in *Mertk* $^{-/-}$ tumors in both CT26 and 4T1 models (p = 0.08) (see Figure 10).

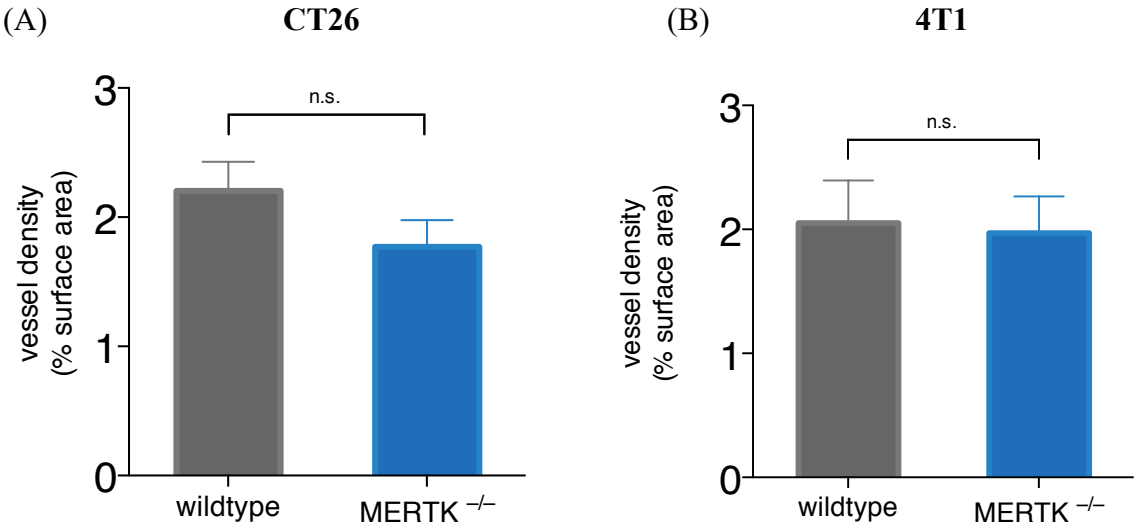

Figure 9 | Immunofluorescent staining of tumor sections does not reveal increased microvascular vessel density. 5 µm sections of size-matched tumors were stained for Endomucin and DAPI. Each area positive for either Endomucin that correlated with positive DAPI-stained nuclei were determined by using *CellProfiler* and represented as Endomucin-positive (% surface area). (A) CT26 colorectal cancer microvascular vessel density (% surface area), n = 6 (B) 4T1 mammary cancer microvascular vessel density (% surface area), n ≥ 4. All data are represented as mean ± SEM. p-value based on one-tailed Student's t-test (n.s. = not significant).

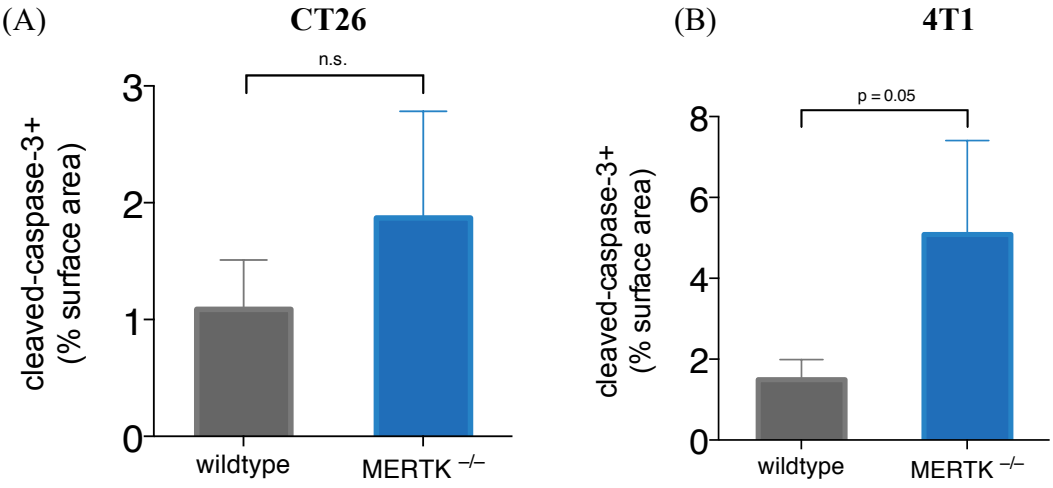

Figure 10| Immunofluorescent staining of tumor sections indicates trend towards increased apoptosis. 5 µm sections of size-matched tumors were stained for cleaved-

caspase-3 and DAPI. Each area positive for either cleaved-caspase-3 that correlated with positive DAPI-stained nuclei were determined by using *CellProfiler* and represented as cleaved-caspase-3-positive (% surface area). (A) CT26 colorectal cancer microvascular vessel density (% surface area), n = 6. (B) 4T1 mammary cancer microvascular vessel density (% surface area), n ≥ 4. All data are represented as mean ± SEM. p-value based on one-tailed Student's t-test (n.s. = not significant).

5.8 Treatment of human macrophages with M6M3 does not lead to MERTK receptor internalization and degradation *in vitro*

In vivo, macrophages exhibit high expression of MERTK (Gautier et al., 2012). We therefore next sought to investigate the effects of M6M3 on THP-1 differentiated human macrophages and their MERTK expression levels via Western Blot. As shown in Figure 11, M6M3 did not induce major MERTK degradation with titrated concentrations of M6M3 at several time points. Additionally, surface expression of MERTK was quantified via flow cytometry and did not reveal a significant difference (see Figure 11).

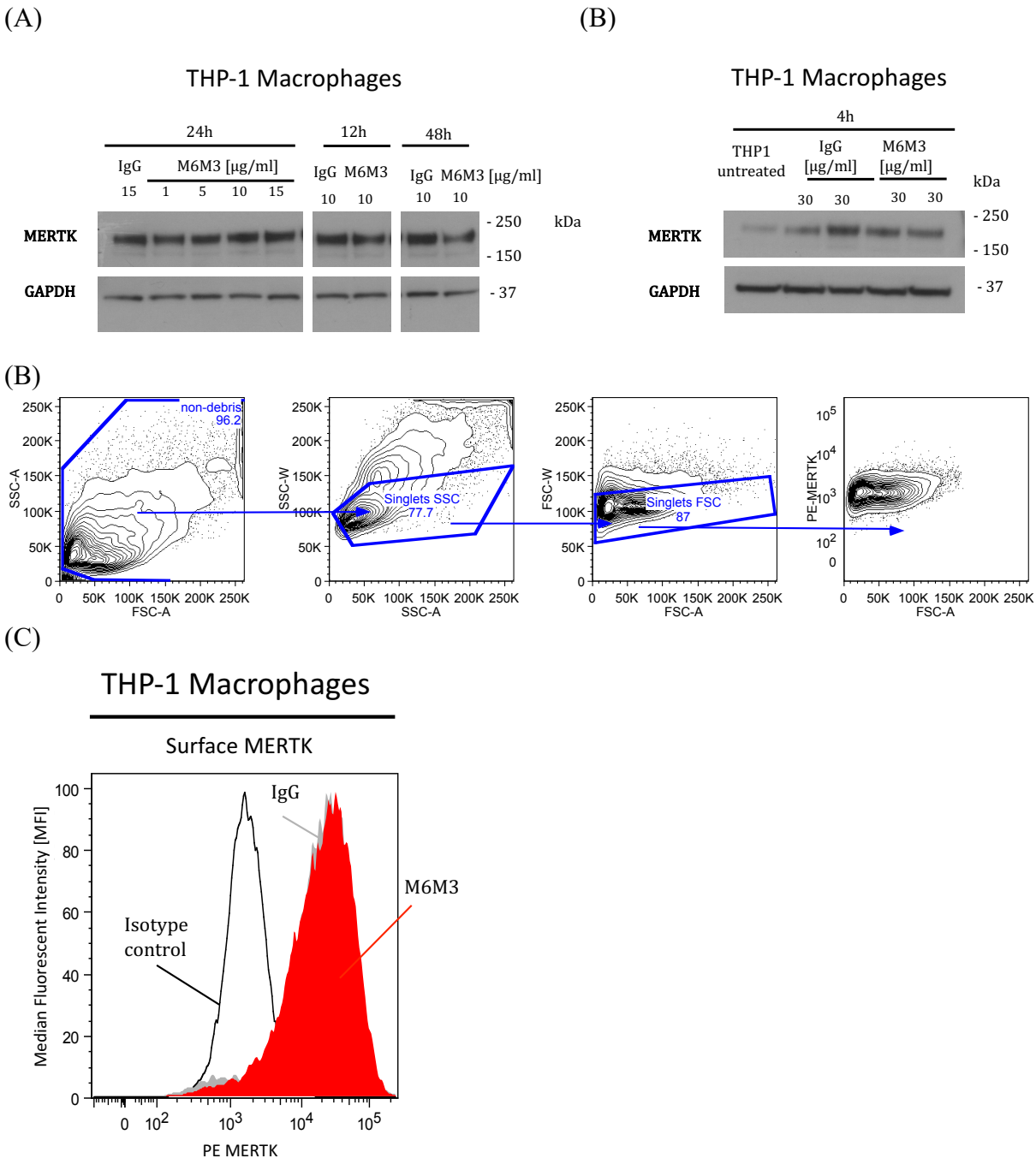

Figure 11| M6M3 did not induce major reduction of total cellular levels of MERTK in human macrophages

(A) THP-1 differentiated macrophages were cultured in the presence of M6M3 or isotype control murine IgG control at different time points (concentrations indicated in annotations). Western blot analysis demonstrated no loss of MERTK protein expression after M6M3. GAPDH was used as a loading control. (B) Gating hierarchy of cells that were analyzed using fluorescent-activated flow cytometry (C) THP-1 differentiated macrophage cultures were treated with 10 µg/ml M6M3 or 10 µg/ml IgG for 16h and then stained for surface expression of MERTK and analyzed by flow cytometry n = 4.

5.9 Treatment of human breast cancer cells with M6M3 does not affect primary tumor growth *in vivo*

After observing robust MERTK degradation in tumor cells *in vitro,* we next assessed the effect of M6M3 on primary tumor growth. Human breast cancer cells MDA-MB-231 were injected orthotopically into immunodeficient mice in two independent experiments. Once tumor volumes reached 100 mm^3 we administered 200µg/mouse of M6M3 3 times a week. No difference in tumor initiation or progression was observed between the M6M3 treated and the control cohort as seen in Figure 12. Similarly, the tumor weight at the end of the experiment did not differ between the groups.

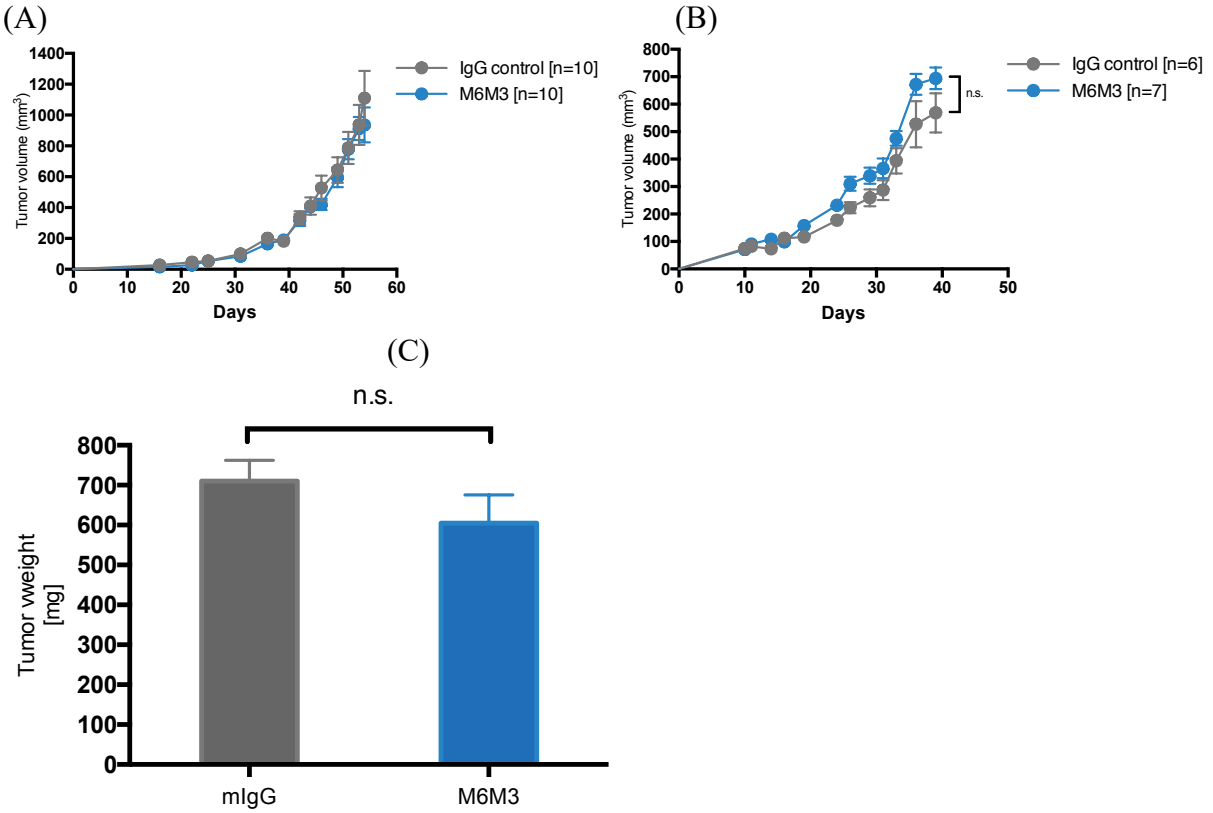

Figure 12| Treatment with M6M3 does not affect primary tumor growth. Two independent primary tumor growth studies of 5 × 10^5 MDA-MB-231 (A) in NOD-scid mice and of (B) 1 × 10^4 MDA-MB-231 in NSG mice injected into the 4th mammary fat pad. n indicated in annotations. Once the average tumor size reached 100 mm^3, each mouse received intraperitoneal injections of 200µg M6M3 or isotype control murine immunoglobulin (IgG) control three times a week. (C) Tumor weights of (A) in a bar chart. n is indicated in figure, all data are represented as mean ± SEM, p-value obtained using a two-sided Student's t-test (n.s. = not significant).

5.10 Treatment of metastatic breast cancer with M6M3 may affect metastatic colonization *in vivo*

Previous studies mainly highlight the impact of MERTK on promoting cancer metastasis (Cook et al., 2013). We thus assessed next a potential impact of the anti-MERTK antibody M6M3 on metastatic progression of breast cancer. To this end, we employed an *in vivo* lung metastasis

model and injected MDA-LM2, the highly metastatic clone of the parental MDA-MB-231, into immunodeficient mice intravenously via the tail vein. Treatment with 200µg/mouse of either M6M3 antibody or IgG control antibody administered intraperitoneal was initiated on the day of implantation. This allowed for the comparison of metastatic progression between anti-MERTK antibody treated and untreated breast cancer cells and to elucidate the colonization capabilities under more physiologic conditions while also refining previous results from our laboratory that investigated MERTK-KD in the metastatic process (Png et al., 2011). Metastatic progression by breast cancer cells was monitored through quantitative bioluminescence imaging. M6M3-treatment decreased the overall growth of metastatic nodules significantly in the initiation growth phase by up to 42% ($p < 0.05$) but no difference was observed after the 18 days' time-point (see Figure 13).

(A)

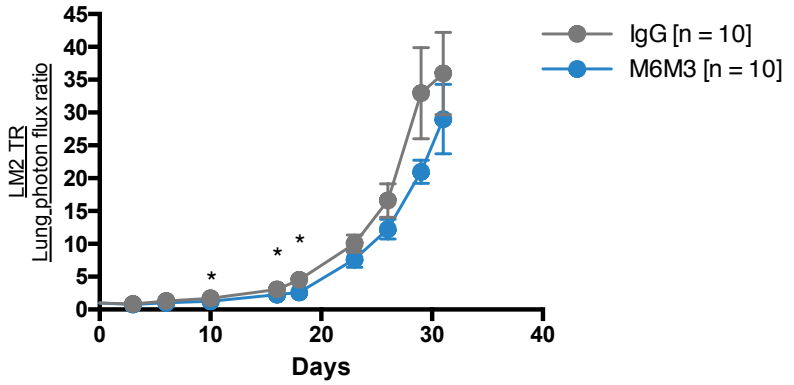

(B)

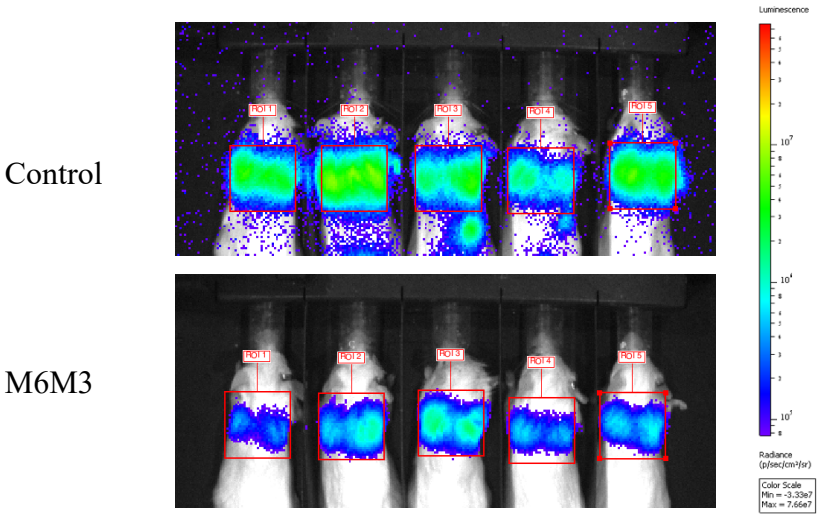

Figure 13| Treatment M6M3 elicits mild effect on metastatic tumor growth.
(A) Bioluminescence imaging plot of lung metastatic colonization by 5×10^4 MDA-LM2 triple reporter cells. Each mouse received intraperitoneal injections of 200µg M6M3 or isotype control murine IgG control three times a week. Treatment was initiated at d = 0. n is indicated in figure and all data are represented as mean ± SEM, p-value obtained using a one-sided Student's t-test (* $p \leq 0.05$). (B) Representative data of *in vivo* imagining using IVIS system, d = 26,

6 Discussion

Cancer is the second leading cause of death worldwide, accounting for an estimated mortality of 9.9 million per year among which breast cancer is ranked second (Ferlay et al., 2021). MERTK expression has repeatedly been reported in multiple tumor entities ranging from hematologic to solid tumors (Graham et al., 2014). In this thesis, we investigated the effects of MERTK on human breast cancer and characterized a novel MERTK-targeting monoclonal antibody, M6M3. As detailed in the previous sections, both *in vitro* and *in vivo* investigations conducted with M6M3 have indicated its potential applicability in breast cancer treatment, but further research is required in order to untangle the complex mechanisms by which cancer utilizes the ability of MERTK and whether M6M3 is fit for clinical application.

6.1 M6M3 antibody development

Previous to this thesis, M6M3 was generated against commercially available human Fc MERTK. Generating an antibody against a commercial and tested protein ensures good reproducibility and reliability in general. For subsequent antibody generation, a hybridoma system was employed. A different anti-MERTK antibody that has proven to have pre-clinical efficacy in non-small cell lung cancer was also produced in this system, supporting the employment of this method (Cummings et al., 2014). Alternatively, a phage display system that has several benefits over the hybridoma technique can be used. In brief, by infecting E.coli with bacteriophages, a library is produced that can also be reused for more antibodies (Clementi et al., 2012). This method is entirely *in vitro*, does not require immunization of animals and is, therefore, less resource- and time-consuming and reduce animal use (Liu, 2014).

The parental hybridoma clones were screened in transwell endothelial recruitment assays and primary tumor growth *in vivo* because previous findings in the Tavazoie laboratory reveal that MERTK-KD via shRNA in tumor cells reduced microvascular vessel density in metastatic nodules of breast cancer (Png et al., 2011). The selection of clone M6M3 was based on its strong binding affinity to MERTK and inhibition of endothelial recruitment *in vitro*.

One of the most critical aspects of a monoclonal antibody is its specific binding to its antigen. Antibody affinity is thereby a centerpiece in defining the potential of M6M3 and that in turn also affects its avidity. M6M3 has shown a very strong affinity exclusively to human MERTK based on previous experiments from the Tavazoie laboratory and was confirmed in ELISA affinity assays (see section 5.1). The selective compatibility to human MERTK allows very distinctive studies of human cancer cells in xenograft models that have a greater proximity to human cancer physiologically. Furthermore, with its high binding affinity, M6M3 only requires concentrations in the nM range in order to detectably bind to its target (see section 5.1). In comparison, Trastuzumab and Pertuzumab exhibit a K_D value of 0.12 and 9.1 nM respectively (Li et al., 2013). A higher affinity also leads to increased antibody dependent cellular cytotoxicity (ADCC) and may increase receptor internalization (Stephen I. Rudnick, 2009). Internalization of an antibody-bound receptor can have both positive and negative effects. On the one hand, the antibody is digested in lysosomes while the receptor can be either recycled or replaced by newly synthesized receptors. Thus, in very large tumors, high antigen densities may act as antibody sinks and prevent deep therapeutic penetration into more distant areas from blood vessels (Keizer et al., 2010, Stone et al., 2014, Wang et al., 2012). On the other hand, sufficient antibody dosages may lead to decreased receptor expression that translates into a long-term inhibition.

A potential downside of high affinity could lead to a "binding site barrier", an observation made by Juweid et al. (Malik Juweid, 1992). This model predicts an inverse relationship between antibody affinity and antibody penetration into a solid tumor. Several studies have proven that the higher the antibody affinity, the less likely it infiltrates into the tumor tissue (Rudnick et al., 2011). Thereby, antigen density on tumor cells as well as vascularization and necrosis influence such effect (Thurber et al., 2008). To overcome the "binding site barrier" adequate dosing is required and may become relevant in designing future *in vivo* or clinical studies.

Another aspect of antibody quality is avidity, the overall strength of an antibody to remain in an associated complex with its antigen. Avidity not only incorporates the antibody affinity but also takes weaker bonds between the antigen and the antibody into consideration. Thus, a higher avidity corresponds to more stability of the antibody-antigen-complex. This may serve as an advantage for M6M3 as results indicate a long-term inhibition of MERTK. The observed MERTK internalization and degradation by Western Blot analysis (see section 5.3) indicates robust avidity. Equally, reduced colony formation *in vitro* evidently demonstrates sustained MERTK inhibition for as long as 10 days after the last treatment. Both strong affinity and avidity can therapeutically be utilized when conjugating M6M3 with a cytotoxic drug such as DM1, a chemotherapeutic agent, coupled to Trastuzumab (Lorusso et al., 2011) that has initiated a range of newly developed antibody-drug conjugates (Ponde et al., 2019).

Another influential immune cell group are Natural Killer T (NKT) cells, that recognize lipid antigens and create an immunoregulatory axis not only promoting anti-tumor immunity but also activating immunosuppressive cells such as regulatory T cells (Tregs) and myeloid-derived suppressor cells (MDSCs) (Terabe and Berzofsky, 2018). For that reason NKT cells are being explored both preclinically and clinically in immunotherapy (Nair and Dhodapkar, 2017). MERTK-KD on NKT cells revealed hyperactivation and secretion of proinflammatory cytokines (Behrens et al., 2003).

6.2 M6M3 treatment efficacy *in vitro*

M6, the parental clone of M6M3, was selected due to its inhibition of angiogenesis *in vitro* and primary tumor growth *in vivo.* In this study, we further characterized the phenotypic effects of M6M3. Treatment with M6M3 (lowest concentration 0.01µg/ml) led to profound MERTK degradation via Western Blot analysis in whole cell lysates. Through fluorescent-activated flow cytometry, we validated reduced expression on the cell surface by ~ 64% ($p = 0.0001$) and in the total cell by 39% ($p = 0.00001$) in the human breast cancer MDA-MB-231 cell line. These findings were comparable to MERTK knock-down levels (Graham et al., 2014) and similar findings in lung cancer (Cummings et al., 2015). The observed increased AXL-levels reactive to M6M3 treatment in MDA-LM2 can be explained by functional rescue by TAM receptor family members utilizing their overlapping binding specifications (Lu et al., 1999). Vice versa, MERTK increases due to pharmacological AXL inhibition in a range of malignancies including TNBC (Mcdaniel et al., 2018). The next anticipated experiment to understand the mechanism of M6M3 better is to perform a Western Blot analysis for changes in phosphorylated (p) pMERTK and its activated downstream signaling proteins pSTAT6, pAKT and pERK after M6M3 treatment. Of note, earlier time points of treatment should be chosen before receptor degradation occurs at 24 h. These results will reveal M6M3's ability to either inhibit, activate or neutralize MERTK signaling.

Interestingly, treatment with M6M3 in THP-1 differentiated human macrophages did not reveal MERTK degradation in Western Blot analysis and fluorescent-activated flow cytometry. We hypothesize that macrophages express higher levels of MERTK than tumor cells and

compensate for the loss of MERTK more efficiently due to their dependence on the receptor especially in the M2 subset (Zizzo et al., 2012). Furthermore, M6M3 binding to MERTK might not lead to receptor internalization in macrophages because it requires the help by cross-linking with co-stimulatory receptors e.g. CD14 and CD32 as these receptors increase efferocytosis (Zizzo and Cohen, 2018). However, it will be interesting to unravel the effects of treatment with M6M3 on MERTK phosphorylation since it could potentially hinder physiologic functions of macrophages such as differentiation or efferocytosis.

Importantly, treatment with M6M3 might lead to undesired MERTK inhibition in a wide range of tissues. Liver-resident macrophages (Kupffer cells) might be greatly affected in their function as immune suppressors since *Mertk* $^{-/-}$ in mice leads to persistent liver injury and inflammation (Triantafyllou et al., 2018). Equally, MERTK is a functional regulator of myelin phagocytosis in brain-resident macrophages (microglia) and its inhibition might affect tissue homeostasis (Nomura et al., 2017) or disease evolution in multiple sclerosis. Furthermore, prolonged MERTK inhibition in humans by mutational loss-of-function induces side effects such as vision changes but arise only after several years (Gal et al., 2000) which is comparable to *Mertk* $^{-/-}$ mice developing retinal pigmentosa (see section 3.2.3). Preliminary data shows disruption of the integrity of the retinal pigmented epithelium in cynomolgus monkeys upon treatment with MERTK-specific antibodies (White et al., 2019). With this question in mind, the humanized M6M3 antibody, called RGX-019, does not elicit any retinal toxicity in cynomolgus monkeys in preliminary data in dosages ranging from 10mg/kg to 100mg/kg (Takeda et al., 2019). Thus, there might be a phase of tolerable therapeutic inhibition in which the advantage of MERTK inhibition outweighs the side effects of M6M3.

The flow cytometry analysis of M6M3-treated MDA-MB-231 cells revealed that the intracellular MERTK signal did not account for the entire quantity of reduced surface receptor expression signal (see section 5.3). This observation might either be due to M6M3 induced receptor internalization and lysosomal degradation or to shedding of the extracellular domain of MERTK by metalloproteinase ADAM17 (Thorp et al., 2011). Png et al. identified MERTK receptor shedding (Png et al., 2011) in MDA-MB-231 cells, however, we suspect MERTK internalization after M6M3 treatment due to higher expression levels on the total cell level than on the surface by ~ 38% ($p \leq 0.000005$). Therefore, upon M6M3 treatment, ~ 39% of total MERTK was either shed as ECD or lysosomally degraded while ~ 23% remained internalized. As there is only one measurement after 24h incubation, further information on the internalized fraction regarding degradation or receptor surface re-integration cannot be given. Additionally, we believe that degradation is the more likely process as a similar anti-MERTK antibody has proven to induce receptor degradation in (Cummings et al., 2014). Receptor shedding could be assessed by e.g. Western Blot analysis of cell culture media of M6M3-treated cells for ECD protein. Nonetheless, loss of MERTK on the cellular surface leads to reduced signaling via the MAPK/ERK, PI3K/AKT and JAK/STAT pathways that affect proliferation/survival as well as transcription (Cummings et al., 2014).

M6M3 treatment did not change the proliferation of tumor cells measured over 6 days. Neither full growth medium nor starvation medium (containing 0.02% FBS) affected this outcome. Although signaling pathways downstream of MERTK affect both proliferation and survival, MERTK tends to promote survival rather than proliferation (Guttridge et al., 2002). Similar to primary tumor growth in *Mertk* $^{-/-}$ hosts being tumor entity specific (see section 5.6) (Crittenden et al., 2016) it can by hypothesized that MERTK inhibition on the tumor cell has varying effects on growth depending on cancer type. For example in gastric cancer, pharmacological MERTK inhibition yielded reduced growth (Kim et al., 2017).

Since Gas6 was initially found in a cDNA library containing genes expressed under conditions of serum deprivation Field (Manfioletti et al., 1993), we hypothesized that MERTK depends on cell survival and growth arrest. Reason for the absence of any effect could be caused by insufficient antibody dosages for the seeding density or ineffective selection pressure by culture conditions such as oxygen concentration or serum starvation. A titration of antibody concentration would therefore determine the optimum amount. Considering the relatively low oxygen levels under which cancer cells in the tumor microenvironment or macrophages in inflamed tissue grow, repeating this experiment under oxygen deprivation or combined with serum starvation could unveil effects on cell viability under hypoxia.

Pretreatment with M6M3 for 72 h resulted in reduced colony formation by 20.4 % ($p=0.0009$) in MDA-MB231 and 11.1% ($p=0.02$) in its highly metastatic subline MDA-LM2 after 10 days. These findings are in agreement with previous observations of loss of MERTK leading to reduced colony formation in other cancer models (Schlegel et al., 2013, Lee-Sherick et al., 2013, Linger et al., 2013). The observed difference in inhibition levels may be due to MDA-LM2 having gained higher expression levels of MERTK and other genes that favor colony formation (Tavazoie et al., 2008). This effect indicates that MERTK is required in the initiation phase of metastatic formation in which single cells acquire the ability to form cell conglomerates in distant sites from the primary tumor. Consequently, it would be interesting to understand whether pre-treatment of cancer cells or the host with M6M3 before transplantation decreases lung metastasis. Furthermore, the lack of MERTK on microenvironmental cells may be disadvantageous for colony formation.

The identified *in vitro* phenotypes indicate promising therapeutic effects that can be utilized to treat cancer. It is therefore interesting to further analyze the efficacy *in vivo* as they offer more physiologic conditions (Weiner, 2010).

With regard to other clinically effective antibodies against RTKs, sufficient attention should be given to receptor activation or inhibition. Theoretically, the two binding sites of a Y-shaped IgG mAb can bind to two independent MERTK receptors. A ∂simultaneous binding to two receptors would theoretically bring them into physical proximity and enable dimerization with subsequent activation of down-stream pathways. This has been well-studied with MET antibodies that lead to transient receptor activation (Prat et al., 1998). Following a short period of receptor activation, internalization and degradation were initiated leading to a long-lasting inhibition of receptor signaling. The fact that M6M3 does not suppress proliferation but suppresses colony formation may indicate that it is an antagonistic mAb in the long-run which has also been concluded from different MET mAb that elicited comparable *in vitro* effects (Prat et al., 1998), but does not rule out initial activation of MERTK subsequent to M6M3 binding.

6.3 The role of MERTK in the tumor microenvironment

Understanding the role of MERTK in the microenvironment and its effects on cancer is crucial in the development of a pharmacological therapy. Studies have shown that efferocytosis creates a supportive microenvironment for tumors and metastasis (Vaught et al., 2015). Efferocytosis of apoptotic tumor cells by M2-polarized macrophages competes with the cell clearance by antigen-presenting cells with higher capacity for immune-stimulatory antigen-presentation, e.g. DCs. MERTK inhibition would theoretically lead to apoptotic cells accumulation in the microenvironment and therefore, increase the chances of antigen uptake by DCs that initiate an anti-tumor immune response. A study by Zhou et al. describes a novel therapeutic anti-MERTK-antibody that blocks efferocytosis on tumor-associated macrophages and thereby

increases tumor immunogenicity, potentiates anti-tumor immunity and decreases tumor growth *in vivo* (Zhou et al., 2020a). This study gives evidence of intercepting efferocytosis as an effective mode of action for an anti-tumor therapy. Testing M6M3 for an equal effect *in vivo* poses a difficult but not insurmountable challenge as M6M3 elicits exclusive specificity towards human and not murine MERTK (see section 5.1). By generating a transgenic mouse with a humanized extracellular domain of MERTK this issue can be overcome. An experimental set up in humanized mice, that contain the human MERTK receptor and its ligands (Gas6 and Pros1) would also be insightful.

Previous investigations in our laboratory led to the hypothesis that MERTK on microenvironmental cells might elicit an anti-tumoral effect. In particular, endothelial MERTK has shown to play a substantial role in endothelial recruitment, a process that is essential for angiogenesis in the tumor microenvironment. Png et al. demonstrated decreased endothelial migration caused by Gas6-dependent MERTK activation on endothelial cells and the abrogation of this phenotype by employment of an anti-MERTK neutralizing antibody (Png et al., 2011). We hypothesized that the overall loss of MERTK in the organism would lead to an increase in angiogenesis and therefore a higher microvascular density in the tumor microenvironment. Furthermore, macrophages induce angiogenesis in a MERTK-dependent manner during the process of tissue repair as anti-inflammatory macrophages are able to secrete VEGF-A (Howangyin et al., 2016). Consistently, there is evidence that MERTK is actively involved in inhibition of angiogenesis. Pros1 inhibits VEGF-A–induced angiogenesis events by activating MERTK and downstream SHP2 (Fraineau et al., 2012). Overexpressed MERTK can inhibit the migration and angiogenesis of human endothelial cells (HMEC-1) through VEGF-C/VEGFR-2 signal pathway (Fan et al., 2007). With this question in mind, immunocompetent *Mertk* $^{-/-}$ mice where challenged with the syngeneic colon cancer CT26 and breast cancer 4T1 cell lines. A reduction in primary tumor growth between the *Mertk* $^{-/-}$ and control group was observed in the CT26 ($p = 0.04$) but not in the 4T1 model. These results may reflect the specificity of different tumor types, suggesting that microenvironmental MERTK has a larger impact on CT26 than on 4T1 cells. Importantly, CT26 is a more immunogenic tumor model than 4T1, potentially indicating that microenvironmental MERTK only exhibits an impact on tumor progression in a context of higher immunoselective pressure. Consistently, in a recent study, *Mertk* deletion impacted growth of CT26 and 4T1 tumors only in combination with radiation therapy, which is known to enhance immunoselective pressure (Crittenden et al., 2016).

We also assessed apoptotic cell burden and microvascular vessel density via immunofluorescent staining in tumors hosted by wildtype and MERTK-knockout mice. Both phenotypes remained unchanged in CT26 and 4T1 between the cohorts, although there was a trend towards increased apoptotic cells in *Mertk* $^{-/-}$ mice. It can therefore be concluded that the reduced primary tumor growth in CT26 neither arises from a difference in vessel density. In regard to other cancer entities, systemic pharmacological MERTK inhibition in glioblastoma correlated with reduced neoangiogenesis *in vivo* (Su et al., 2020) indicating a positive effect of MERTK inhibition on endothelial cells. Taken together, these results implicate a negligible effect of MERTK in the tumor microenvironment on the 4T1 model exhibiting low and a modest impact on the more immunogenic CT26 model.

For future directions it would be informative to analyze the effects of an anti-MERTK antibody directed at murine MERTK that could be employed in animal experiments with syngeneic tumor models in immune-competent mice. As MERTK is expressed in numerous cell types, it is of particular interest to observe the effect of MERTK inhibition both in the tumor and its

microenvironment. mAb-mediated inhibition of MERTK on tumor-associated M2 – macrophages leads to the inhibition of efferocytosis of apoptotic cancer cells and the secretion of interferon-β (Zhou et al., 2020a). As characterized in section 3.3.4, MERTK inhibition on $CD11b^+$ cells would further support an anti-tumor response by prolonging a proinflammatory reaction (Cook et al., 2013, Paolino and Penninger, 2016). Additionally, Pros1 expression on human T cells activates AXL and MERTK on DCs and thereby inhibits their activation as a negative feedback loop which could be interrupted by antibody-associated MERTK inhibition (Carrera Silva et al., 2013).

6.4 M6M3 characterization *in vivo*

The additional validation and characterization of the efficacy of M6M3 *in vivo* was of crucial importance. Although MERTK was found in human breast cancer to drive metastasis (Tavazoie et al., 2008, Png et al., 2011) and M6M3 was chosen for its strong inhibition of angiogenesis by endothelial recruitment in metastasis, we were curious to assess the effect of M6M3 on primary tumor growth. For that purpose, we transplanted human breast cancer cells MDA-MB-231 orthotopically into NOD-SCID mice, an immunodeficient mouse model, and intravenously administered one cohort with M6M3 and the other cohort with isotype control mIgG. Primary tumor growth was unaffected by M6M3 treatment after termination of the experiment. We repeated the experiment and used the NSG mouse model, which exhibits more severe immunodeficiency than NOD-SCID. We confirmed that M6M3 treatment does not elicit any effect on primary tumor growth. Doses of 1.0 mg/injection/mouse of comparable antibodies (Cetuximab, Trastuzumab) have shown to penetrate MDA-MB-231 tumors more homogenously overall (Lee and Tannock, 2010). Hence, a potential improvement to the experimental design is the administration of higher dosages from 200µg to 500 µg – 1.0 mg of M6M3. Furthermore, pretreating tumor cells with M6M3 could have given further indications about its effect on MERTK activity on tumor cells. It is also worthwhile to further investigate this phenotype with a more MERTK-dependent tumor model that could be more sensitive to M6M3 such as human non-small cell lung cancer (Shengzhi Xie, 2015).

Next, we observed that M6M3 has a growth-inhibiting effect in the initiation phase (days 10 – 18) in metastatic tumor growth assays ($p > 0.05$) via bioluminescent *in vivo* measurement. These results reflect the impaired colony formation phenotype observed *in vitro*. Nevertheless, this effect was not preserved after the 18 days-time-point which may indicate a compensation mechanism by the tumor. A possible approach to solve this problem is by increasing antibody dosage (Lee and Tannock, 2010) or application frequency to ensure an effective tissue penetration by the antibody. It is also worth pursuing a different experimental endpoint such as overall survival. Furthermore, treating the same target with two pharmacological agents may lead to increased inhibition. Mer590, an anti-MERTK antibody currently in the preclinical phase, in combination with small-hairpin ribonucleic acid (shRNA) against MERTK has shown to have enhanced treatment effect (Cummings et al., 2014). Equally, antibodies are often given in combination with chemotherapy, such as trastuzumab + epirubicin + docetaxel (Venturini et al., 2006). Comparably, the combination of anti-MERTK mAb in combination with PD-1 inhibition and radiotherapy promotes abscopal antitumor Immune responses in lung adenocarcinoma xenografts by improving tumor immunogenicity (Caetano et al., 2019).

6.5 Translating M6M3 to patients

M6M3 is a murine antibody. Importantly, to advance its use as a therapeutic in humans, at least partial humanization would be required. Humanization involves the exchange of the Fc portion

of a chimeric antibody from murine to human. Importantly, the IgG subclass (IgG1 - IgG4) should be chosen reasonably rationally as different subclasses lead to different activation of CDC or ADCC (Kretschmer et al., 2017). So far, most mAbs in cancer therapy have an IgG1 Fc-region. In comparison, IgG3 is equally effective activating ADCC but elicits the highest binding to C1q to promote CDC. Thus, humanizing M6M3 with an IgG3 Fc-region could not only impair MERTK function but also lead to effective anti-tumor immune activation. Notably, previously reported production issues and reduced serum half-life of IgG3 (7 days compared to 21 days of IgG1) should also be considered (Bonilla, 2008), (Kretschmer et al., 2017). However, Stapleton and colleagues have successfully increased serum-half life by amino-acid exchange at position 435 (Stapleton et al., 2011). Furthermore, engineering the heavy chains by Fc mutagenesis creating asymmetrical Fc portions as heterodimers resulted in more stable antibodies with enhanced ADCC efficacy (Liu et al., 2014). Especially, Afucosylation, the process of removing fucose sugar from the glycolysation patterns of the Fc-region yielded a 50-fold boost in ADCC (Liu et al., 2015). Chimeric antibodies, in which only the Fc antibody region is humanized, such as Rituximab, can be employed in cancer therapy, but they show significant levels of immunogenicity. Studies report the development of human anti-mouse-antibodies (HAMAs), as an immune response to chimeric mAb, in up to 50% of cases of treated patients (Azinovic et al., 2006). In order to further reduce immunogenicity, antibodies should ideally be fully humanized, which would also entail humanizing the antibody scaffold in the variable region surrounding the complementarity-determining region (Riechmann et al., 1988, Tan et al., 2002)

Antibody-drug-conjugates (ADC), mAb conjugated to cytotoxic agents, have gained increased attention in the recent years. Utilizing the high specificity of antibodies against their antigens can be utilized for precise and concentrated drug delivery to the tumor. In fluorescent activated flow cytometry analysis, we have observed M6M3 inducing robust MERTK internalization. This phenotype can be very beneficial when cytotoxic drugs can enter tumor cells through this mechanism. In fact, studies have proven a positive correlation between antibody affinity and promotion of receptor internalization (Rudnick et al., 2011, Opalinski et al., 2018). Both strong affinity and avidity of M6M3 (see section 5.1) can therapeutically be utilized when conjugating M6M3 to a cytotoxic drug. A potential candidate is DM1, a chemotherapeutic agent, that has proven effective when coupled to Trastuzumab (Lorusso et al., 2011) and initiated a range of newly developed antibody-drug conjugates (Ponde et al., 2019)

7 Summary

Cancer is the second leading cause of death worldwide accounting for an estimated mortality of 9.9 million per year (Ferlay et al., 2021) among which breast cancer is ranked second (Bray et al., 2018). MERTK expression has repeatedly been reported in multiple tumor entities ranging from hematologic to solid tumors (Graham et al., 2014). This study investigated the effects of MERTK and characterized M6M3, a novel MERTK-targeting monoclonal antibody, in human breast cancer.

We validated strong affinity of M6M3 exclusively to human MERTK in ELISA affinity assays. Treatment with M6M3 led to profound MERTK degradation via Western Blot analysis. Through fluorescent-activated flow cytometry, we demonstrated reduced expression on the cell surface. Direct inhibition of cancer cell proliferation upon M6M3 treatment could not be detected. However, pretreatment with M6M3 resulted in significantly reduced colony formation.

In order to assess effects of MERTK in the microenvironment, immunocompetent *Mertk* $^{-/-}$ mice where challenged with the syngeneic colon cancer CT26 and breast cancer 4T1 cell lines. A reduction in primary tumor growth was detected between the *Mertk* $^{-/-}$ and control group depending on the cancer entity. Apoptotic cell burden and neoangiogenesis were unaffected by *Mertk* $^{-/-}$.

With the aim to assess the direct therapeutic efficacy *in vivo* we transplanted the human breast cancer cell line MDA-MB-231 into an immunodeficient mouse model and administered intravenously one cohort with M6M3 and the other cohort with isotype control mIgG. Orthotopic primary tumor growth after termination of the experiment was unaffected by M6M3 treatment. Next, we transplanted the metastatic derivative cell line MDA-LM2 in a metastatic tumor growth assays and observed that M6M3 treatment has a significant growth-inhibiting effect in the initiation phase (days 10 – 18) via bioluminescent *in vivo* measurement. This finding indicates a higher dependency on MERTK in metastatic formation.

The studies presented in this thesis showed promising pre-clinical results in support of targeting MERTK therapeutically. Both *in vitro* and *in vivo* experiments conducted with M6M3 have demonstrated phenotypic effects on MERTK. Thus, M6M3 shows potential as a cancer therapy candidate that may be translated into clinical application.

German/Deutsch:

Krebs ist die zweithäufigste Todesursache weltweit mit einer geschätzten Sterblichkeit von 9,9 Millionen pro Jahr (Ferlay et al., 2021), wobei Brustkrebs an zweiter Stelle steht (Bray et al., 2018). Die Expression von MERTK wurde wiederholt in verschiedenen Tumorentitäten, von hämatologischen bis hin zu soliden Tumoren festgestellt (Graham et al., 2014). In dieser Dissertation wurden die Auswirkungen von MERTK untersucht und *M6M3*, ein neuartiger MERTK-spezifischer monoklonaler Antikörper in menschlichem Brustkrebs charakterisiert.

In ELISA-Affinitäts-Assays konnten wir eine hohe Affinität von M6M3 ausschließlich zu menschlichem MERTK nachweisen. Die Behandlung mit M6M3 führte zu einem signifikanten MERTK-Abbau mittels Western-Blot-Analyse. Mittels fluoreszenzaktivierter Durchflusszytometrie konnten wir eine reduzierte Expression auf der Zelloberfläche nachweisen. Eine direkte Hemmung der Proliferation von Krebszellen durch die Behandlung mit M6M3 konnte nicht festgestellt werden. Die Vorbehandlung mit M6M3 führte jedoch zu einer deutlich reduzierten Koloniebildung.

Um die Auswirkungen von MERTK auf die Mikroumgebung zu untersuchen, wurden immunkompetente Mertk -/- Mäuse mit den syngenen Darmkrebs- CT26- und Brustkrebs-Zelllinien 4T1 befallen. Je nach Krebsart wurde eine Verringerung des Primärtumorwachstums zwischen der Mertk -/- und der Kontrollgruppe festgestellt. Die apoptotische Zelllast und die Neoangiogenese wurden durch Mertk -/- nicht beeinträchtigt.

Um die direkte therapeutische Wirksamkeit in vivo zu untersuchen, transplantierten wir die humane Brustkrebszelllinie MDA-MB-231 in ein immundefizientes Mausmodell und verabreichten einer Kohorte intravenös *M6M3* und der anderen Kohorte die Isotyp-Kontrolle mIgG. Das Wachstum des orthotopen Primärtumors nach Beendigung des Experiments wurde durch die *M6M3*-Behandlung nicht beeinflusst. Als Nächstes transplantierten wir die metastasierende Zelllinie MDA-LM2 in einem metastasierenden Tumorwachstumstest und beobachteten, dass die Behandlung mit M6M3 in der Initiationsphase (Tage 10 - 18) mittels biolumineszenter in-vivo-Messung eine signifikante wachstumshemmende Wirkung hat. Dieser Befund deutet auf eine stärkere Abhängigkeit von MERTK bei der Metastasenbildung hin.

Die in dieser Arbeit vorgestellten Ergebnisse zeigen vielversprechende präklinische Ergebnisse, die einen therapeutischen Ansatz gegen MERTK unterstützen. Sowohl *in vitro* als auch *in vivo* durchgeführte Experimente mit *M6M3* haben phänotypische Auswirkungen auf MERTK gezeigt. Somit zeigt *M6M3* Potenzial als Krebstherapiekandidat, der in die klinische Anwendung überführt werden kann.

8 List of Abbreviations

AC	apoptotic cells
ADC	Antibody -drug-conjugates
ADCC	antibody-dependent cell-mediated cytotoxicity
AJCC	American Joint Commission on Cancer
APC	antigen-presenting cells
ATCC	American Type Tissue Collection
bp	base pairs
CDC	complement-dependent cytotoxicity
Ct	Cycles to Threshold
CTCs	circulating tumor cells
DC	dendritic cell
ECD	extracellular domain
EGF	epidermal growth factor
EGFR	epithelial growth-factor receptor
EMA	European Medicines Agency
EMT	epithelial-mesenchymal-transition
ER	estrogen receptor
FACS	Fluorescence-activated flow cytometry
FBS	Fetal bovine serum
FDA	Food and Drug Administration
Gas6	growth arrest specific factor 6
GOI	Gene of interest
h	Hour(s)
HAMAs	human anti-mouse-antibodies
HER2	human epidermal growth factor receptor 2
hMer-DDDK	human MERTK bound to DDDK-tag
hMer-Fc	human MERTK bound to human antibody Fc-part
HNSCC	head and neck squamous cell carcinoma
IACUC	Institutional Animal Care and Use Committee
IgG	Immunoglobuline G
IL	interleukin
mAbs	monoclonal antibodies
MAPK	MAP kinase
Mer –/–	Mertk-knockout
MERTK	Myeloid-epithelial-reproductive tyrosine kinase
MERTK-KD	MERTK knock-down
MET	mesenchymal-epithelial-transition
mIgG	Murine Immunuglobuline G
min	Minute(s)
miRNA	microRNA

mM	millimolar
mMer-Fc	murine MERTK bound to human antibody Fc-part
MVD	microvessel density
NKT	natural killer T
nM	nanomolar
NOD	non-obese diabetic
norm	normalization
NSCLC	Non-small cell lung cancer
NSG	NOD-*scid*, NOD-*scid* IL2Rgamma^{null}
p	phosphorylated
PAF	platelet-activating factor
PAMPS	Pathogen-associated molecular patterns
PBS	phosphate buffered saline
PCR	Polymerase chain reaction
PGE2	prostaglandin E2
PMA	with phorbol 12-myristate-13-acetate
PR	progesteron receptor
Pros1	Protein S
PtdSer	phosphatidyl serine
qPCR	Quantitative polymerase chain reaction
RT	Room temperature
RT-PCR	Reverse transcription polymerase chain reaction
RTKs	receptor tyrosine kinases
SHBG	sex hormone binding globulin domain
shRNA	small-hairpin ribonucleic acid
sMer	soluble MERTK
TAM	TYRO-AXL-MERTK
TAM TKO	*Tyro3* $^{-/-}$ *Axl* $^{-/-}$ *Mertk* $^{-/-}$ triple-knock-out
TGFβ	transforming growth factor-beta
TNBC	Triple negative breast cancer
TNF-α	tumor necrosis factor-alpha
TULP1	tubby-like protein 1
UICC	Union for International Cancer Control
VEGF	vascular endothelial growth factor
VEGF-A	vascular endothelial growth factor A
VEGFR2	vascular endothelial growth factor receptor 2
wt	wildtype

9 Bibliography

A.G.N. 1931. The Late Baron Shibasaburo Kitasato. *Can Med Assoc J,* 25**,** 206.

Abboud-Jarrous, G., Priya, S., Maimon, A., Fischman, S., Cohen-Elisha, M., Czerninski, R. & Burstyn-Cohen, T. 2017. Protein S drives oral squamous cell carcinoma tumorigenicity through regulation of AXL. *Oncotarget,* 8**,** 13986-14002.

Aceto, N., Bardia, A., Miyamoto, D. T., Donaldson, M. C., Wittner, B. S., Spencer, J. A., Yu, M., Pely, A., Engstrom, A., Zhu, H., Brannigan, B. W., Kapur, R., Stott, S. L., Shioda, T., Ramaswamy, S., Ting, D. T., Lin, C. P., Toner, M., Haber, D. A. & Maheswaran, S. 2014. Circulating tumor cell clusters are oligoclonal precursors of breast cancer metastasis. *Cell,* 158**,** 1110-1122.

American-Cancer-Society 2019. Cancer Facts & Figures 2019.

Angelillo-Scherrer, A., de Frutos, P., Aparicio, C., Melis, E., Savi, P., Lupu, F., Arnout, J., Dewerchin, M., Hoylaerts, M., Herbert, J., Collen, D., Dahlbäck, B. & Carmeliet, P. 2001. Deficiency or inhibition of Gas6 causes platelet dysfunction and protects mice against thrombosis. *Nat Med,* 7**,** 215-21.

Au, S. H., Storey, B. D., Moore, J. C., Tang, Q., Chen, Y.-L., Javaid, S., Sarioglu, A. F., Sullivan, R., Madden, M. W., O'Keefe, R., Haber, D. A., Maheswaran, S., Langenau, D. M., Stott, S. L. & Toner, M. 2016. Clusters of circulating tumor cells traverse capillary-sized vessels. *Proceedings of the National Academy of Sciences,* 113**,** 4947.

Azad, T., Nouri, K., Janse van Rensburg, H. J., Maritan, S. M., Wu, L., Hao, Y., Montminy, T., Yu, J., Khanal, P., Mulligan, L. M. & Yang, X. 2020. A gain-of-functional screen identifies the Hippo pathway as a central mediator of receptor tyrosine kinases during tumorigenesis. *Oncogene,* 39**,** 334-355.

Azinovic, I., DeNardo, G. L., Lamborn, K. R., Mirick, G., Goldstein, D., Bradt, B. M. & DeNardo, S. J. 2006. Survival benefit associated with human anti-mouse antibody (HAMA) in patients with B-cell malignancies. *Cancer Immunol Immunother,* 55**,** 1451-8.

Behrens, E. M., Gadue, P., Gong, S. Y., Garrett, S., Stein, P. L. & Cohen, P. L. 2003. The mer receptor tyrosine kinase: expression and function suggest a role in innate immunity. *Eur J Immunol,* 33**,** 2160-7.

Bonilla, F. A. 2008. Pharmacokinetics of immunoglobulin administered via intravenous or subcutaneous routes. *Immunol Allergy Clin North Am,* 28**,** 803-19, ix.

Bosurgi, L., Bernink, J. H., Delgado Cuevas, V., Gagliani, N., Joannas, L., Schmid, E. T., Booth, C. J., Ghosh, S. & Rothlin, C. V. 2013. Paradoxical role of the proto-oncogene Axl and Mer receptor tyrosine kinases in colon cancer. *Proceedings of the National Academy of Sciences,* 110**,** 13091.

Boyd, N. F., Dite, G. S., Stone, J., Gunasekara, A., English, D. R., McCredie, M. R., Giles, G. G., Tritchler, D., Chiarelli, A., Yaffe, M. J. & Hopper, J. L. 2002. Heritability of mammographic density, a risk factor for breast cancer. *N Engl J Med,* 347**,** 886-94.

Boyd, N. F., Martin, L. J., Yaffe, M. J. & Minkin, S. 2011. Mammographic density and breast cancer risk: current understanding and future prospects. *Breast Cancer Res,* 13**,** 223.

Brabletz, T., Kalluri, R., Nieto, M. A. & Weinberg, R. A. 2018. EMT in cancer. *Nat Rev Cancer,* 18**,** 128-134.

Bray, F., Ferlay, J., Soerjomataram, I., Siegel, R. L., Torre, L. A. & Jemal, A. 2018. Global cancer statistics 2018: GLOBOCAN estimates of incidence and mortality worldwide for 36 cancers in 185 countries. *CA: A Cancer Journal for Clinicians,* 68**,** 394-424.

Burstyn-Cohen, T. 2017. TAM receptor signaling in development. *Int J Dev Biol,* 61**,** 215-224.
Caberoy, N. B., Alvarado, G., Bigcas, J. L. & Li, W. 2012. Galectin-3 is a new MerTK-specific eat-me signal. *J Cell Physiol,* 227**,** 401-7.
Caberoy, N. B., Zhou, Y. & Li, W. 2010. Tubby and tubby-like protein 1 are new MerTK ligands for phagocytosis. *Embo j,* 29**,** 3898-910.
Caetano, M. S., Younes, A. I., Barsoumian, H. B., Quigley, M., Menon, H., Gao, C., Spires, T., Reilly, T. P., Cadena, A. P., Cushman, T. R., Schoenhals, J. E., Li, A., Nguyen, Q.-N., Cortez, M. A. & Welsh, J. W. 2019. Triple Therapy with MerTK and PD1 Inhibition Plus Radiotherapy Promotes Abscopal Antitumor Immune Responses. *Clinical Cancer Research,* 25**,** 7576.
Caiazza, F., McGowan, P. M., Mullooly, M., Murray, A., Synnott, N., O'Donovan, N., Flanagan, L., Tape, C. J., Murphy, G., Crown, J. & Duffy, M. J. 2015. Targeting ADAM-17 with an inhibitory monoclonal antibody has antitumour effects in triple-negative breast cancer cells. *Br J Cancer,* 112**,** 1895-903.
Camenisch, T. D., Koller, B. H., Earp, H. S. & Matsushima, G. K. 1999. A novel receptor tyrosine kinase, Mer, inhibits TNF-alpha production and lipopolysaccharide-induced endotoxic shock. *J Immunol,* 162**,** 3498-503.
Carrera Silva, E. A., Chan, P. Y., Joannas, L., Errasti, A. E., Gagliani, N., Bosurgi, L., Jabbour, M., Perry, A., Smith-Chakmakova, F., Mucida, D., Cheroutre, H., Burstyn-Cohen, T., Leighton, J. A., Lemke, G., Ghosh, S. & Rothlin, C. V. 2013. T cell-derived protein S engages TAM receptor signaling in dendritic cells to control the magnitude of the immune response. *Immunity,* 39**,** 160-70.
Chambers, A. F., Groom, A. C. & MacDonald, I. C. 2002. Dissemination and growth of cancer cells in metastatic sites. *Nat Rev Cancer,* 2**,** 563-72.
Chen, C., Li, Q., Darrow, A. L., Wang, Y., Derian, C. K., Yang, J., de Garavilla, L., Andrade-Gordon, P. & Damiano, B. P. 2004. Mer receptor tyrosine kinase signaling participates in platelet function. *Arterioscler Thromb Vasc Biol,* 24**,** 1118-23.
Chiang, A. C. & Massagué, J. 2008. Molecular basis of metastasis. *N Engl J Med,* 359**,** 2814-23.
Clementi, N., Mancini, N., Solforosi, L., Castelli, M., Clementi, M. & Burioni, R. 2012. Phage display-based strategies for cloning and optimization of monoclonal antibodies directed against human pathogens. *Int J Mol Sci,* 13**,** 8273-92.
Clynes, R. A., Towers, T. L., Presta, L. G. & Ravetch, J. V. 2000. Inhibitory Fc receptors modulate in vivo cytoxicity against tumor targets. *Nature Medicine,* 6**,** 443-446.
Cook, D. & Swayne, D. F. 2007. *Interactive and Dynamic Graphics for Data Analysis: With Examples Using R and GGobi: Springer*.
Cook, R. S., Jacobsen, K. M., Wofford, A. M., DeRyckere, D., Stanford, J., Prieto, A. L., Redente, E., Sandahl, M., Hunter, D. M., Strunk, K. E., Graham, D. K. & Earp, H. S., 3rd 2013. MerTK inhibition in tumor leukocytes decreases tumor growth and metastasis. *J Clin Invest,* 123**,** 3231-42.
Crittenden, M. R., Baird, J., Friedman, D., Savage, T., Uhde, L., Alice, A., Cottam, B., Young, K., Newell, P., Nguyen, C., Bambina, S., Kramer, G., Akporiaye, E., Malecka, A., Jackson, A. & Gough, M. J. 2016. Mertk on tumor macrophages is a therapeutic target to prevent tumor recurrence following radiation therapy. *Oncotarget,* 7**,** 78653-78666.
Cummings, C. T., Deryckere, D., Earp, H. S. & Graham, D. K. 2013. Molecular pathways: MERTK signaling in cancer. *Clin Cancer Res,* 19**,** 5275-80.
Cummings, C. T., Linger, R. M., Cohen, R. A., Sather, S., Kirkpatrick, G. D., Davies, K. D., DeRyckere, D., Earp, H. S. & Graham, D. K. 2014. Mer590, a novel monoclonal

antibody targeting MER receptor tyrosine kinase, decreases colony formation and increases chemosensitivity in non-small cell lung cancer. *Oncotarget,* 5**,** 10434-45.

Cummings, C. T., Zhang, W., Davies, K. D., Kirkpatrick, G. D., Zhang, D., DeRyckere, D., Wang, X., Frye, S. V., Earp, H. S. & Graham, D. K. 2015. Small Molecule Inhibition of MERTK Is Efficacious in Non-Small Cell Lung Cancer Models Independent of Driver Oncogene Status. *Mol Cancer Ther,* 14**,** 2014-22.

Davra, V., Kumar, S., Geng, K., Calianese, D., Mehta, D., Gadiyar, V., Kasikara, C., Lahey, K. C., Chang, Y. J., Wichroski, M., Gao, C., De Lorenzo, M. S., Kotenko, S. V., Bergsbaken, T., Mishra, P. K., Gause, W. C., Quigley, M., Spires, T. E. & Birge, R. B. 2021. Axl and Mertk Receptors Cooperate to Promote Breast Cancer Progression by Combined Oncogenic Signaling and Evasion of Host Antitumor Immunity. *Cancer Res,* 81**,** 698-712.

Du, W., Zhu, J., Zeng, Y., Liu, T., Zhang, Y., Cai, T., Fu, Y., Zhang, W., Zhang, R., Liu, Z. & Huang, J. A. 2021. KPNB1-mediated nuclear translocation of PD-L1 promotes non-small cell lung cancer cell proliferation via the Gas6/MerTK signaling pathway. *Cell Death Differ,* 28**,** 1284-1300.

Du, Z. & Lovly, C. M. 2018. Mechanisms of receptor tyrosine kinase activation in cancer. *Molecular Cancer,* 17**,** 58.

Duncan, J. L., LaVail, M. M., Yasumura, D., Matthes, M. T., Yang, H., Trautmann, N., Chappelow, A. V., Feng, W., Earp, H. S., Matsushima, G. K. & Vollrath, D. 2003. An RCS-like retinal dystrophy phenotype in mer knockout mice. *Invest Ophthalmol Vis Sci,* 44**,** 826-38.

Elliott, M. R. & Ravichandran, K. S. 2016. The Dynamics of Apoptotic Cell Clearance. *Dev Cell,* 38**,** 147-60.

Fadok, V. A., Bratton, D. L., Konowal, A., Freed, P. W., Westcott, J. Y. & Henson, P. M. 1998. Macrophages that have ingested apoptotic cells in vitro inhibit proinflammatory cytokine production through autocrine/paracrine mechanisms involving TGF-beta, PGE2, and PAF. *Journal of Clinical Investigation,* 101**,** 890-898.

Fan, L., Zhou, M. Y., Shen, F., Xie, L. Q. & Ruan, C. G. 2007. [Effect of Mer overexpression on HMEC-1 cell angiogenesis and its mechanism]. *Zhonghua Xue Ye Xue Za Zhi,* 28**,** 602-4.

Ferlay, J., Colombet, M., Soerjomataram, I., Parkin, D. M., Piñeros, M., Znaor, A. & Bray, F. 2021. Cancer statistics for the year 2020: An overview. *Int J Cancer*.

Ferlay J, S. I., Ervik M, Dikshit R, Eser S, Mathers C 2012. Cancer Incidence and Mortality Worldwide: IARC CancerBase No. 11. *GLOBOCAN 2012 v1.0*.

Fidler, I. J. 2003. The pathogenesis of cancer metastasis: the 'seed and soil' hypothesis revisited.

Fraineau, S., Monvoisin, A., Clarhaut, J., Talbot, J., Simonneau, C., Kanthou, C., Kanse, S. M., Philippe, M. & Benzakour, O. 2012. The vitamin K-dependent anticoagulant factor, protein S, inhibits multiple VEGF-A-induced angiogenesis events in a Mer- and SHP2-dependent manner. *Blood,* 120**,** 5073-5083.

Franken, N. A. P., Rodermond, H. M., Stap, J., Haveman, J. & van Bree, C. 2006. Clonogenic assay of cells in vitro. *Nature Protocols,* 1**,** 2315.

Friguet, B., Chaffotte, A. F., Djavadi-Ohaniance, L. & Goldberg, M. E. 1985. Measurements of the true affinity constant in solution of antigen-antibody complexes by enzyme-linked immunosorbent assay. *J Immunol Methods,* 77**,** 305-19.

Gal, A., Li, Y., Thompson, D. A., Weir, J., Orth, U., Jacobson, S. G., Apfelstedt-Sylla, E. & Vollrath, D. 2000. Mutations in MERTK, the human orthologue of the RCS rat retinal dystrophy gene, cause retinitis pigmentosa. *Nature Genetics,* 26**,** 270.

Ganesh, K. & Massague, J. 2021. Targeting metastatic cancer. *Nat Med,* 27**,** 34-44.

Gautier, E. L., Shay, T., Miller, J., Greter, M., Jakubzick, C., Ivanov, S., Helft, J., Chow, A., Elpek, K. G., Gordonov, S., Mazloom, A. R., Ma'ayan, A., Chua, W.-J., Hansen, T. H., Turley, S. J., Merad, M., Randolph, G. J., Gautier, E. L., Jakubzick, C., Randolph, G. J., Best, A. J., Knell, J., Goldrath, A., Miller, J., Brown, B., Merad, M., Jojic, V., Koller, D., Cohen, N., Brennan, P., Brenner, M., Shay, T., Regev, A., Fletcher, A., Elpek, K., Bellemare-Pelletier, A., Malhotra, D., Turley, S., Jianu, R., Laidlaw, D., Collins, J., Narayan, K., Sylvia, K., Kang, J., Gazit, R., Garrison, B. S., Rossi, D. J., Kim, F., Rao, T. N., Wagers, A., Shinton, S. A., Hardy, R. R., Monach, P., Bezman, N. A., Sun, J. C., Kim, C. C., Lanier, L. L., Heng, T., Kreslavsky, T., Painter, M., Ericson, J., Davis, S., Mathis, D., Benoist, C. & the Immunological Genome, C. 2012. Gene-expression profiles and transcriptional regulatory pathways that underlie the identity and diversity of mouse tissue macrophages. *Nature Immunology,* 13**,** 1118-1128.

Geyer, F. C., Marchio, C. & Reis-Filho, J. S. 2009. The role of molecular analysis in breast cancer. *Pathology,* 41**,** 77-88.

Gianni, L., Pienkowski, T., Im, Y.-H., Roman, L., Tseng, L.-M., Liu, M.-C., Lluch, A., Staroslawska, E., de la Haba-Rodriguez, J., Im, S.-A., Pedrini, J. L., Poirier, B., Morandi, P., Semiglazov, V., Srimuninnimit, V., Bianchi, G., Szado, T., Ratnayake, J., Ross, G. & Valagussa, P. 2012. Efficacy and safety of neoadjuvant pertuzumab and trastuzumab in women with locally advanced, inflammatory, or early HER2-positive breast cancer (NeoSphere): a randomised multicentre, open-label, phase 2 trial. *The Lancet Oncology,* 13**,** 25-32.

Gilmour, M., Scholtz, A., Ottmann, O. G., Hills, R. K., Knapper, S. & Zabkiewicz, J. 2016. Axl/ Mer Inhibitor ONO-9330547 As a Novel Therapeutic Agent in a Stromal Co-Culture Model of Primary Acute Myeloid Leukaemia (AML). *Blood,* 128**,** 2754.

Graham, D. K., Dawson, T. L., Mullaney, D. L., Snodgrass, H. R. & Earp, H. S. 1994. Cloning and mRNA expression analysis of a novel human protooncogene, c-mer. *Cell Growth Differ,* 5**,** 647-57.

Graham, D. K., DeRyckere, D., Davies, K. D. & Earp, H. S. 2014. The TAM family: phosphatidylserine sensing receptor tyrosine kinases gone awry in cancer. *Nat Rev Cancer,* 14**,** 769-85.

Gschwind, A., Fischer, O. M. & Ullrich, A. 2004. The discovery of receptor tyrosine kinases: targets for cancer therapy. *Nat Rev Cancer,* 4**,** 361-70.

Guttridge, K. L., Luft, J. C., Dawson, T. L., Kozlowska, E., Mahajan, N. P., Varnum, B. & Earp, H. S. 2002. Mer receptor tyrosine kinase signaling: prevention of apoptosis and alteration of cytoskeletal architecture without stimulation or proliferation. *J Biol Chem,* 277**,** 24057-66.

Hajdu, S. I. 2011. A note from history: Landmarks in history of cancer, part 1. *Cancer,* 117**,** 1097-1102.

Hedemann, N., Rogmans, C., Sebens, S., Wesch, D., Reichert, M., Schmidt-Arras, D., Oberg, H. H., Pecks, U., van Mackelenbergh, M., Weimer, J., Arnold, N., Maass, N. & Bauerschlag, D. O. 2018. ADAM17 inhibition enhances platinum efficiency in ovarian cancer. *Oncotarget,* 9**,** 16043-16058.

Hill, A. A. C., Jacqueline; DeRyckere, Deborah; Graham, Douglas K 2015. The MERTK Signalling Pathway in Cancer. *eLS*.

Howangyin, K. Y., Zlatanova, I., Pinto, C., Ngkelo, A., Cochain, C., Rouanet, M., Vilar, J., Lemitre, M., Stockmann, C., Fleischmann, B. K., Mallat, Z. & Silvestre, J. S. 2016. Myeloid-Epithelial-Reproductive Receptor Tyrosine Kinase and Milk Fat Globule Epidermal Growth Factor 8 Coordinately Improve Remodeling After Myocardial

Infarction via Local Delivery of Vascular Endothelial Growth Factor. *Circulation,* 133**,** 826-39.
Howlader, N. N., AM; Krapcho, M; Miller, D; Brest, A; Yu, M; Ruhl, J; Tatalovich, Z; Mariotto, A; Lewis, DR; Chen, HS; Feuer, EJ; Cronin, KA (eds). 2016. https://seer.cancer.gov/csr/1975_2016/, based on November 2018 SEER data submission, posted to the SEER web site, accessed April 2019.
Hu, Z., Li, Z., Ma, Z. & Curtis, C. 2020. Multi-cancer analysis of clonality and the timing of systemic spread in paired primary tumors and metastases. *Nature genetics,* 52**,** 701-708.
Huynh, M.-L. N., Fadok, V. A. & Henson, P. M. 2002. Phosphatidylserine-dependent ingestion of apoptotic cells promotes TGF-β1 secretion and the resolution of inflammation. *The Journal of Clinical Investigation,* 109**,** 41-50.
Jiang, Y., Zhang, Y., Leung, J. Y., Fan, C., Popov, K. I., Su, S., Qian, J., Wang, X., Holtzhausen, A., Ubil, E., Xiang, Y., Davis, I., Dokholyan, N. V., Wu, G., Perou, C. M., Kim, W. Y., Earp, H. S. & Liu, P. 2019. MERTK mediated novel site Akt phosphorylation alleviates SAV1 suppression. *Nat Commun,* 10**,** 1515.
Jing, Y., Han, Z., Zhang, S., Liu, Y. & Wei, L. 2011. Epithelial-Mesenchymal Transition in tumor microenvironment. *Cell & bioscience,* 1**,** 29-29.
Joosse, S. A., Gorges, T. M. & Pantel, K. 2015. Biology, detection, and clinical implications of circulating tumor cells. *EMBO molecular medicine,* 7**,** 1-11.
Jun Ho Yi, J. J., Jeonghee Cho, In-Gu Do3, Mineui Hong4, Seung Tae Kim1, Kyoung-Mee Kim4, Sujin Lee1, Se Hoon Park1, Joon Oh Park1,4, Young Suk Park1, Won Ki Kang1, Ho Yeong Lim1, Jeeyun Lee 2015. MerTK is a novel therapeutic target in gastric cancer. *Oncotarget*.
Kalluri, R. & Weinberg, R. A. 2009. The basics of epithelial-mesenchymal transition. *J Clin Invest,* 119**,** 1420-8.
Kasikara, C., Davra, V., Calianese, D., Geng, K., Spires, T. E., Quigley, M., Wichroski, M., Sriram, G., Suarez-Lopez, L., Yaffe, M. B., Kotenko, S. V., De Lorenzo, M. S. & Birge, R. B. 2019. Pan-TAM Tyrosine Kinase Inhibitor BMS-777607 Enhances Anti-PD-1 mAb Efficacy in a Murine Model of Triple-Negative Breast Cancer. *Cancer Res,* 79**,** 2669-2683.
Keating, A. K., Kim, G. K., Jones, A. E., Donson, A. M., Ware, K., Mulcahy, J. M., Salzberg, D. B., Foreman, N. K., Liang, X., Thorburn, A. & Graham, D. K. 2010. Inhibition of Mer and Axl receptor tyrosine kinases in astrocytoma cells leads to increased apoptosis and improved chemosensitivity. *Mol Cancer Ther,* 9**,** 1298-307.
Keizer, R. J., Huitema, A. D., Schellens, J. H. & Beijnen, J. H. 2010. Clinical pharmacokinetics of therapeutic monoclonal antibodies. *Clin Pharmacokinet,* 49**,** 493-507.
Kim, J. E., Kim, Y., Li, G., Kim, S. T., Kim, K., Park, S. H., Park, J. O., Park, Y. S., Lim, H. Y., Lee, H., Sohn, T. S., Kim, K. M., Kang, W. K. & Lee, J. 2017. MerTK inhibition by RXDX-106 in MerTK activated gastric cancer cell lines. *Oncotarget,* 8**,** 105727-105734.
Knubel KH, B. M. P., Alexandra Sufit1, Sarah Nelson1, Angela M. Pierce1, Amy K. Keating1 2014. MerTK inhibition is a novel therapeutic approach for glioblastoma multiforme.
Kretschmer, A., Schwanbeck, R., Valerius, T. & Rosner, T. 2017. Antibody Isotypes for Tumor Immunotherapy. *Transfus Med Hemother,* 44**,** 320-326.
Lai, C. & Lemke, G. 1991. An extended family of protein-tyrosine kinase genes differentially expressed in the vertebrate nervous system. *Neuron,* 6**,** 691-704.
Lambert, A. W., Pattabiraman, D. R. & Weinberg, R. A. 2017. Emerging Biological Principles of Metastasis. *Cell,* 168**,** 670-691.

Lee, C. M. & Tannock, I. F. 2010. The distribution of the therapeutic monoclonal antibodies cetuximab and trastuzumab within solid tumors. *Bmc Cancer,* 10.

Lee-Sherick, A. B., Eisenman, K. M., Sather, S., McGranahan, A., Armistead, P. M., McGary, C. S., Hunsucker, S. A., Schlegel, J., Martinson, H., Cannon, C., Keating, A. K., Earp, H. S., Liang, X., DeRyckere, D. & Graham, D. K. 2013. Aberrant Mer receptor tyrosine kinase expression contributes to leukemogenesis in acute myeloid leukemia. *Oncogene,* 32**,** 5359-68.

Lemke, G. 2013. Biology of the TAM receptors. *Cold Spring Harb Perspect Biol,* 5**,** a009076.

Lemke, G. & Burstyn-Cohen, T. 2010. TAM receptors and the clearance of apoptotic cells. *Ann N Y Acad Sci,* 1209**,** 23-9.

Lemke, G. & Rothlin, C. V. 2008. Immunobiology of the TAM receptors. *Nat Rev Immunol,* 8**,** 327-36.

Li, B., Meng, Y., Zheng, L., Zhang, X., Tong, Q., Tan, W., Hu, S., Li, H., Chen, Y., Song, J., Zhang, G., Zhao, L., Zhang, D., Hou, S., Qian, W. & Guo, Y. 2013. Bispecific antibody to ErbB2 overcomes trastuzumab resistance through comprehensive blockade of ErbB2 heterodimerization. *Cancer Res,* 73**,** 6471-83.

Li, T., Sun, L., Miller, N., Nicklee, T., Woo, J., Hulse-Smith, L., Tsao, M. S., Khokha, R., Martin, L. & Boyd, N. 2005. The association of measured breast tissue characteristics with mammographic density and other risk factors for breast cancer. *Cancer Epidemiol Biomarkers Prev,* 14**,** 343-9.

Li, Y., Wang, X., Bi, S., Zhao, K. & Yu, C. 2015. Inhibition of Mer and Axl receptor tyrosine kinases leads to increased apoptosis and improved chemosensitivity in human neuroblastoma. *Biochemical and Biophysical Research Communications,* 457**,** 461-466.

Linderholm, B., Lindh, B., Tavelin, B., Grankvist, K. & Henriksson, R. 2000. p53 and vascular-endothelial-growth-factor (VEGF) expression predicts outcome in 833 patients with primary breast carcinoma. *Int J Cancer,* 89**,** 51-62.

Lindsay, R. S., Whitesell, J. C., Dew, K. E., Rodriguez, E., Sandor, A. M., Tracy, D., Yannacone, S. F., Basta, B. N., Jacobelli, J. & Friedman, R. S. 2021. MERTK on mononuclear phagocytes regulates T cell antigen recognition at autoimmune and tumor sites. *J Exp Med,* 218.

Ling, L., Templeton, D. & Kung, H. J. 1996. Identification of the major autophosphorylation sites of Nyk/Mer, an NCAM-related receptor tyrosine kinase. *J Biol Chem,* 271**,** 18355-62.

Linger, R. M., Cohen, R. A., Cummings, C. T., Sather, S., Migdall-Wilson, J., Middleton, D. H., Lu, X., Baron, A. E., Franklin, W. A., Merrick, D. T., Jedlicka, P., DeRyckere, D., Heasley, L. E. & Graham, D. K. 2013. Mer or Axl receptor tyrosine kinase inhibition promotes apoptosis, blocks growth and enhances chemosensitivity of human non-small cell lung cancer. *Oncogene,* 32**,** 3420-31.

Linger, R. M., Keating, A. K., Earp, H. S. & Graham, D. K. 2008. TAM receptor tyrosine kinases: biologic functions, signaling, and potential therapeutic targeting in human cancer. *Adv Cancer Res,* 100**,** 35-83.

Liu, J. K. 2014. The history of monoclonal antibody development - Progress, remaining challenges and future innovations. *Ann Med Surg (Lond),* 3**,** 113-6.

Liu, S. D., Chalouni, C., Young, J. C., Junttila, T. T., Sliwkowski, M. X. & Lowe, J. B. 2015. Afucosylated Antibodies Increase Activation of FcγRIIIa-Dependent Signaling Components to Intensify Processes Promoting ADCC. *Cancer Immunology Research,* 3**,** 173.

Liu, Z., Gunasekaran, K., Wang, W., Razinkov, V., Sekirov, L., Leng, E., Sweet, H., Foltz, I., Howard, M., Rousseau, A. M., Kozlosky, C., Fanslow, W. & Yan, W. 2014.

Asymmetrical Fc engineering greatly enhances antibody-dependent cellular cytotoxicity (ADCC) effector function and stability of the modified antibodies. *J Biol Chem,* 289**,** 3571-90.

Loh, H.-Y., Norman, B. P., Lai, K.-S., Rahman, N. M. A. N. A., Alitheen, N. B. M. & Osman, M. A. 2019. The Regulatory Role of MicroRNAs in Breast Cancer. *International journal of molecular sciences,* 20**,** 4940.

Longatto Filho, A., Lopes, J. M. & Schmitt, F. C. 2010. Angiogenesis and breast cancer. *Journal of oncology,* 2010**,** 576384.

LoRusso, P. M., Weiss, D., Guardino, E., Girish, S. & Sliwkowski, M. X. 2011. Trastuzumab emtansine: a unique antibody-drug conjugate in development for human epidermal growth factor receptor 2-positive cancer. *Clin Cancer Res,* 17**,** 6437-47.

Lu, Q., Gore, M., Zhang, Q., Camenisch, T., Boast, S., Casagranda, F., Lai, C., Skinner, M. K., Klein, R., Matsushima, G. K., Earp, H. S., Goff, S. P. & Lemke, G. 1999. Tyro-3 family receptors are essential regulators of mammalian spermatogenesis. *Nature,* 398**,** 723-8.

Maimon, A., Levi-Yahid, V., Ben-Meir, K., Halpern, A., Talmi, Z., Priya, S., Mizraji, G., Mistriel-Zerbib, S., Berger, M., Baniyash, M., Loges, S. & Burstyn-Cohen, T. 2021. Myeloid cell-derived PROS1 inhibits tumor metastasis by regulating inflammatory and immune responses via IL-10. *J Clin Invest,* 131.

Malik Juweid, R. N., Chaing Paik, Miguel J. Perez-Bacete, Jun Sato, William van Osdol, and John N. Weinstein1 1992. Micropharmacology of Monoclonal Antibodies in Solid Tumors: Direct Experimental Evidence for a Binding Site Barrier. *Cancer Res*.

Mark, M. R., Chen, J., Hammonds, R. G., Sadick, M. & Godowsk, P. J. 1996. Characterization of Gas6, a member of the superfamily of G domain-containing proteins, as a ligand for Rse and Axl. *Journal of Biological Chemistry,* 271**,** 9785-9789.

Martineau, P. 2010. Affinity Measurements by Competition ELISA. *Antibody Engineering.*

Massague, J. & Obenauf, A. C. 2016. Metastatic colonization by circulating tumour cells. *Nature,* 529**,** 298-306.

McDaniel, N. K., Cummings, C. T., Iida, M., Hülse, J., Pearson, H. E., Vasileiadi, E., Parker, R. E., Orbuch, R. A., Ondracek, O. J., Welke, N. B., Kang, G. H., Davies, K. D., Wang, X., Frye, S. V., Earp, H. S., Harari, P. M., Kimple, R. J., DeRyckere, D., Graham, D. K. & Wheeler, D. L. 2018. MERTK Mediates Intrinsic and Adaptive Resistance to AXL-targeting Agents. *Mol Cancer Ther,* 17**,** 2297-2308.

Migdall-Wilson, J., Bates, C., Schlegel, J., Brandao, L., Linger, R. M., DeRyckere, D. & Graham, D. K. 2012. Prolonged exposure to a Mer ligand in leukemia: Gas6 favors expression of a partial Mer glycoform and reveals a novel role for Mer in the nucleus. *PLoS One,* 7**,** e31635.

Minn, A. J., Gupta, G. P., Siegel, P. M., Bos, P. D., Shu, W., Giri, D. D., Viale, A., Olshen, A. B., Gerald, W. L. & Massagué, J. 2005. Genes that mediate breast cancer metastasis to lung. *Nature,* 436**,** 518-24.

Mittal, S., Brown, N. J. & Holen, I. 2018. The breast tumor microenvironment: role in cancer development, progression and response to therapy. *Expert Rev Mol Diagn,* 18**,** 227-243.

Mukherjee, S. 2010. The Emperor of All Maladies.

Myers, K. V., Amend, S. R. & Pienta, K. J. 2019. Targeting Tyro3, Axl and MerTK (TAM receptors): implications for macrophages in the tumor microenvironment. *Mol Cancer,* 18**,** 94.

Nagata, K., Ohashi, K., Nakano, T., Arita, H., Zong, C., Hanafusa, H. & Mizuno, K. 1996. Identification of the product of growth arrest-specific gene 6 as a common ligand for Axl, Sky, and Mer receptor tyrosine kinases. *Journal of Biological Chemistry,* 271**,** 30022-30027.

Nair, S. & Dhodapkar, M. V. 2017. Natural Killer T Cells in Cancer Immunotherapy. *Frontiers in immunology,* 8**,** 1178-1178.

Nguyen, D. X., Bos, P. D. & Massagué, J. 2009. Metastasis: from dissemination to organ-specific colonization. *Nat Rev Cancer,* 9**,** 274-84.

Nguyen, K. Q., Tsou, W. I., Calarese, D. A., Kimani, S. G., Singh, S., Hsieh, S., Liu, Y., Lu, B., Wu, Y., Garforth, S. J., Almo, S. C., Kotenko, S. V. & Birge, R. B. 2014. Overexpression of MERTK receptor tyrosine kinase in epithelial cancer cells drives efferocytosis in a gain-of-function capacity. *J Biol Chem,* 289**,** 25737-49.

Nguyen, K. Q., Tsou, W. I., Kotenko, S. & Birge, R. B. 2013. TAM receptors in apoptotic cell clearance, autoimmunity, and cancer. *Autoimmunity,* 46**,** 294-7.

Nomura, K., Vilalta, A., Allendorf, D. H., Hornik, T. C. & Brown, G. C. 2017. Activated Microglia Desialylate and Phagocytose Cells via Neuraminidase, Galectin-3, and Mer Tyrosine Kinase. *Journal of immunology (Baltimore, Md. : 1950),* 198**,** 4792-4801.

Novitskiy, S. V., Zaynagetdinov, R., Vasiukov, G., Gutor, S., Han, W., Serezani, A., Matafonov, A., Gleaves, L. A., Sherrill, T. P., Polosukhin, V. V. & Blackwell, T. S. 2019. Gas6/MerTK signaling is negatively regulated by NF-κB and supports lung carcinogenesis. *Oncotarget,* 10**,** 7031-7042.

Ohashi, K., Nagata, K., Toshima, J., Nakano, T., Arita, H., Tsuda, H., Suzuki, K. & Mizuno, K. 1995. Stimulation of sky receptor tyrosine kinase by the product of growth arrest-specific gene 6. *J Biol Chem,* 270**,** 22681-4.

Olea-Flores, M., Zuñiga-Eulogio, M. D., Mendoza-Catalán, M. A., Rodríguez-Ruiz, H. A., Castañeda-Saucedo, E., Ortuño-Pineda, C., Padilla-Benavides, T. & Navarro-Tito, N. 2019. Extracellular-Signal Regulated Kinase: A Central Molecule Driving Epithelial-Mesenchymal Transition in Cancer. *International journal of molecular sciences,* 20**,** 2885.

Opalinski, L., Szymczyk, J., Szczepara, M., Kucinska, M., Krowarsch, D., Zakrzewska, M. & Otlewski, J. 2018. High Affinity Promotes Internalization of Engineered Antibodies Targeting FGFR1. *Int J Mol Sci,* 19.

Paget, S. 1889. THE DISTRIBUTION OF SECONDARY GROWTHS IN CANCER OF THE BREAST. *The Lancet,* 133**,** 571-573.

Paolino, M. & Penninger, J. M. 2016. The Role of TAM Family Receptors in Immune Cell Function: Implications for Cancer Therapy. *Cancers (Basel),* 8.

Pastore, M., Grimaudo, S., Pipitone, R. M., Lori, G., Raggi, C., Petta, S. & Marra, F. 2019. Role of Myeloid-Epithelial-Reproductive Tyrosine Kinase and Macrophage Polarization in the Progression of Atherosclerotic Lesions Associated With Nonalcoholic Fatty Liver Disease. *Frontiers in Pharmacology,* 10.

Png, K. J., Halberg, N., Yoshida, M. & Tavazoie, S. F. 2011. A microRNA regulon that mediates endothelial recruitment and metastasis by cancer cells. *Nature,* 481**,** 190-4.

Ponde, N., Aftimos, P. & Piccart, M. 2019. Antibody-Drug Conjugates in Breast Cancer: a Comprehensive Review. *Curr Treat Options Oncol,* 20**,** 37.

Ponomarev, V., Doubrovin, M., Serganova, I., Vider, J., Shavrin, A., Beresten, T., Ivanova, A., Ageyeva, L., Tourkova, V., Balatoni, J., Bornmann, W., Blasberg, R. & Gelovani Tjuvajev, J. 2004. A novel triple-modality reporter gene for whole-body fluorescent, bioluminescent, and nuclear noninvasive imaging. *European Journal of Nuclear Medicine and Molecular Imaging,* 31**,** 740-751.

Pradip Sen, M. A. W., 1 Zuoan Yi,1 Yingsu Huang,1 Michael Henderson,1 Clayton E. Mathews,2 H. Shelton Earp,3,4 Glenn Matsushima,1,3,5 Albert S. Baldwin Jr,3,6 and Roland M. Tisch1,3 2007. Apoptotic cells induce Mer tyrosine kinase–dependent blockade of NF- B activation in dendritic cells.

Prasad, D., Rothlin, C. V., Burrola, P., Burstyn-Cohen, T., Lu, Q., Garcia de Frutos, P. & Lemke, G. 2006. TAM receptor function in the retinal pigment epithelium. *Mol Cell Neurosci,* 33**,** 96-108.

Prat, M., Crepaldi, T., Pennacchietti, S., Bussolino, F. & Comoglio, P. M. 1998. Agonistic monoclonal antibodies against the Met receptor dissect the biological responses to HGF. *J Cell Sci,* 111 (Pt 2)**,** 237-47.

Rahman, Z. S., Shao, W. H., Khan, T. N., Zhen, Y. & Cohen, P. L. 2010. Impaired apoptotic cell clearance in the germinal center by Mer-deficient tingible body macrophages leads to enhanced antibody-forming cell and germinal center responses. *J Immunol,* 185**,** 5859-68.

Reiter, J. G., Makohon-Moore, A. P., Gerold, J. M., Heyde, A., Attiyeh, M. A., Kohutek, Z. A., Tokheim, C. J., Brown, A., DeBlasio, R. M., Niyazov, J., Zucker, A., Karchin, R., Kinzler, K. W., Iacobuzio-Donahue, C. A., Vogelstein, B. & Nowak, M. A. 2018. Minimal functional driver gene heterogeneity among untreated metastases. *Science (New York, N.Y.),* 361**,** 1033-1037.

Riechmann, L., Clark, M., Waldmann, H. & Winter, G. 1988. Reshaping human antibodies for therapy. *Nature,* 332**,** 323-327.

Rogers, A. E., Le, J. P., Sather, S., Pernu, B. M., Graham, D. K., Pierce, A. M. & Keating, A. K. 2012. Mer receptor tyrosine kinase inhibition impedes glioblastoma multiforme migration and alters cellular morphology. *Oncogene,* 31**,** 4171-81.

Rudnick, S. I., Lou, J., Shaller, C. C., Tang, Y., Klein-Szanto, A. J., Weiner, L. M., Marks, J. D. & Adams, G. P. 2011. Influence of affinity and antigen internalization on the uptake and penetration of Anti-HER2 antibodies in solid tumors. *Cancer Res,* 71**,** 2250-9.

Ruvolo, P. P., Ma, H., Ruvolo, V. R., Zhang, X., Mu, H., Schober, W., Hernandez, I., Gallardo, M., Khoury, J. D., Cortes, J., Andreeff, M. & Post, S. M. 2017. Anexelekto/MER tyrosine kinase inhibitor ONO-7475 arrests growth and kills FMS-like tyrosine kinase 3-internal tandem duplication mutant acute myeloid leukemia cells by diverse mechanisms. *Haematologica,* 102**,** 2048-2057.

Saraon, P., Musrap, N., Cretu, D., Karagiannis, G. S., Batruch, I., Smith, C., Drabovich, A. P., Trudel, D., van der Kwast, T., Morrissey, C., Jarvi, K. A. & Diamandis, E. P. 2012. Proteomic profiling of androgen-independent prostate cancer cell lines reveals a role for protein S during the development of high grade and castration-resistant prostate cancer. *J Biol Chem,* 287**,** 34019-31.

Sather, S., Kenyon, K. D., Lefkowitz, J. B., Liang, X. Y., Varnum, B. C., Henson, P. M. & Graham, D. K. 2007. A soluble form of the Mer receptor tyrosine kinase inhibits macrophage clearance of apoptotic cells and platelet aggregation. *Blood,* 109**,** 1026-1033.

Schlegel, J., Sambade, M. J., Sather, S., Moschos, S. J., Tan, A. C., Winges, A., DeRyckere, D., Carson, C. C., Trembath, D. G., Tentler, J. J., Eckhardt, S. G., Kuan, P. F., Hamilton, R. L., Duncan, L. M., Miller, C. R., Nikolaishvili-Feinberg, N., Midkiff, B. R., Liu, J., Zhang, W., Yang, C., Wang, X., Frye, S. V., Earp, H. S., Shields, J. M. & Graham, D. K. 2013. MERTK receptor tyrosine kinase is a therapeutic target in melanoma. *J Clin Invest,* 123**,** 2257-67.

Scott, R. S., McMahon, E. J., Pop, S. M., Reap, E. A., Caricchio, R., Cohen, P. L., Earp, H. S. & Matsushima, G. K. 2001. Phagocytosis and clearance of apoptotic cells is mediated by MER. *Nature,* 411**,** 207-211.

Senkus, E., Kyriakides, S., Ohno, S., Penault-Llorca, F., Poortmans, P., Rutgers, E., Zackrisson, S., Cardoso, F. & Committee, E. G. 2015. Primary breast cancer: ESMO Clinical

Practice Guidelines for diagnosis, treatment and follow-up. *Ann Oncol,* 26 Suppl 5**,** v8-30.

Shaver, T. M., Lehmann, B. D., Beeler, J. S., Li, C. I., Li, Z., Jin, H., Stricker, T. P., Shyr, Y. & Pietenpol, J. A. 2016. Diverse, Biologically Relevant, and Targetable Gene Rearrangements in Triple-Negative Breast Cancer and Other Malignancies. *Cancer Res,* 76**,** 4850-60.

Shelby, S. J., Feathers, K. L., Ganios, A. M., Jia, L., Miller, J. M. & Thompson, D. A. 2015. MERTK signaling in the retinal pigment epithelium regulates the tyrosine phosphorylation of GDP dissociation inhibitor alpha from the GDI/CHM family of RAB GTPase effectors. *Exp Eye Res,* 140**,** 28-40.

Shengzhi Xie, Y. L., Xiaoyan Li, Linxiong Wang, Na Yang, Yadi Wang, Huafeng Wei 2015. Mer receptor tyrosine kinase is frequently overexpressed in human non-small cell lung cancer, confirming resistance to erlotinib.

Shi, C., Li, X., Wang, X., Ding, N., Ping, L., Shi, Y., Mi, L., Lai, Y., Song, Y. & Zhu, J. 2018. The proto-oncogene Mer tyrosine kinase is a novel therapeutic target in mantle cell lymphoma. *J Hematol Oncol,* 11**,** 43.

Stapleton, N. M., Andersen, J. T., Stemerding, A. M., Bjarnarson, S. P., Verheul, R. C., Gerritsen, J., Zhao, Y., Kleijer, M., Sandlie, I., de Haas, M., Jonsdottir, I., van der Schoot, C. E. & Vidarsson, G. 2011. Competition for FcRn-mediated transport gives rise to short half-life of human IgG3 and offers therapeutic potential. *Nat Commun,* 2**,** 599.

Stephen I. Rudnick, G. P. A. 2009. Affinity and Avidity in Antibody-Based Tumor Targeting. *CANCER BIOTHERAPY AND RADIOPHARMACEUTICALS*.

Stevens, F. J. 1987. Modification of an Elisa-Based Procedure for Affinity Determination - Correction Necessary for Use with Bivalent Antibody. *Molecular Immunology,* 24**,** 1055-1060.

Stone, R. H., Hong, J. & Jeong, H. 2014. Pharmacokinetics of monoclonal antibodies used for inflammatory bowel diseases in pregnant women. *Journal of clinical toxicology,* 4**,** 209.

Su, Y.-T., Butler, M., Zhang, M., Zhang, W., Song, H., Hwang, L., Tran, A. D., Bash, R. E., Schorzman, A. N., Pang, Y., Yu, G., Zamboni, W. C., Wang, X., Frye, S. V., Miller, C. R., Maric, D., Terabe, M., Gilbert, M. R., Earp Iii, H. S. & Wu, J. 2020. MerTK inhibition decreases immune suppressive glioblastoma-associated macrophages and neoangiogenesis in glioblastoma microenvironment. *Neuro-Oncology Advances,* 2.

Suarez, R. M., Chevot, F., Cavagnino, A., Saettel, N., Radvanyi, F., Piguel, S., Bernard-Pierrot, I., Stoven, V. & Legraverend, M. 2013. Inhibitors of the TAM subfamily of tyrosine kinases: synthesis and biological evaluation. *Eur J Med Chem,* 61**,** 2-25.

Takeda, S., Andreu-Agullo, C., Sridhar, S., Halberg, N., Lorenz, I. C., Tavazoie, S., Kurth, I. & Tavazoie, M. 2019. Abstract LB-277: Characterization of the anti-cancer and immunologic activity of RGX-019, a novel pre-clinical stage humanized monoclonal antibody targeting the MERTK receptor. *Cancer Research,* 79**,** LB-277.

Tan, P., Mitchell, D. A., Buss, T. N., Holmes, M. A., Anasetti, C. & Foote, J. 2002. "Superhumanized" Antibodies: Reduction of Immunogenic Potential by Complementarity-Determining Region Grafting with Human Germline Sequences: Application to an Anti-CD28. *The Journal of Immunology,* 169**,** 1119.

Tavazoie, S. F., Alarcon, C., Oskarsson, T., Padua, D., Wang, Q., Bos, P. D., Gerald, W. L. & Massague, J. 2008. Endogenous human microRNAs that suppress breast cancer metastasis. *Nature,* 451**,** 147-52.

Terabe, M. & Berzofsky, J. A. 2018. Tissue-Specific Roles of NKT Cells in Tumor Immunity. *Frontiers in immunology,* 9**,** 1838-1838.

Thorp, E., Vaisar, T., Subramanian, M., Mautner, L., Blobel, C. & Tabas, I. 2011. Shedding of the Mer tyrosine kinase receptor is mediated by ADAM17 protein through a pathway involving reactive oxygen species, protein kinase Cdelta, and p38 mitogen-activated protein kinase (MAPK). *J Biol Chem,* 286**,** 33335-44.

Thurber, G. M., Schmidt, M. M. & Wittrup, K. D. 2008. Antibody tumor penetration: transport opposed by systemic and antigen-mediated clearance. *Adv Drug Deliv Rev,* 60**,** 1421-34.

TN Stitt, G. C., Martin Gore,, Cary Lai, J. B., * Czeslaw Radziejewski,* Karen Mattsson,* John Fisher,* David R. Gies,* Pamela F. Jones,* Piotr Masiakowski,*, Terence E. Ryan, N. J. T., * D. H. Chen,* Peter S. DiStefano,* George L. Long,II & Claudio Basilico, M. P. G., * Greg Lemke,t David J. Glass,* and George D. Yancopoulos* 1995. The Anticoagulation Factor Protein S and Its Relative, Gas6, Are Ligandsfor the Tyro 3/Axl Family of Receptor Tyrosine Kinases.

Triantafyllou, E., Pop, O. T., Possamai, L. A., Wilhelm, A., Liaskou, E., Singanayagam, A., Bernsmeier, C., Khamri, W., Petts, G., Dargue, R., Davies, S. P., Tickle, J., Yuksel, M., Patel, V. C., Abeles, R. D., Stamataki, Z., Curbishley, S. M., Ma, Y., Wilson, I. D., Coen, M., Woollard, K. J., Quaglia, A., Wendon, J., Thursz, M. R., Adams, D. H., Weston, C. J. & Antoniades, C. G. 2018. MerTK expressing hepatic macrophages promote the resolution of inflammation in acute liver failure. *Gut,* 67**,** 333-347.

Tsang, J. Y. S. & Tse, G. M. 2020. Molecular Classification of Breast Cancer. *Adv Anat Pathol,* 27**,** 27-35.

Tsou, W. I., Nguyen, K. Q., Calarese, D. A., Garforth, S. J., Antes, A. L., Smirnov, S. V., Almo, S. C., Birge, R. B. & Kotenko, S. V. 2014. Receptor tyrosine kinases, TYRO3, AXL, and MER, demonstrate distinct patterns and complex regulation of ligand-induced activation. *J Biol Chem,* 289**,** 25750-63.

U.S. National Library of Medicine 2020. Clinicaltrials.gov, https://clinicaltrials.gov/ct2/results?cond=Cancer&term=mertk&cntry=&state=&city=&dist= (accessed 3 Jul 2020).

Ubil, E., Caskey, L., Holtzhausen, A., Hunter, D., Story, C. & Earp, H. S. 2018. Tumor-secreted Pros1 inhibits macrophage M1 polarization to reduce antitumor immune response. *J Clin Invest,* 128**,** 2356-2369.

Uehara, H. & Shacter, E. 2008. Auto-Oxidation and Oligomerization of Protein S on the Apoptotic Cell Surface Is Required for Mer Tyrosine Kinase-Mediated Phagocytosis of Apoptotic Cells. *The Journal of Immunology,* 180**,** 2522-2530.

Ursin, G., Hovanessian-Larsen, L., Parisky, Y. R., Pike, M. C. & Wu, A. H. 2005. Greatly increased occurrence of breast cancers in areas of mammographically dense tissue. *Breast Cancer Res,* 7**,** R605-8.

Vaught, D. B., Stanford, J. C. & Cook, R. S. 2015. Efferocytosis creates a tumor microenvironment supportive of tumor survival and metastasis. *Cancer Cell Microenviron,* 2.

Venturini, M., Bighin, C., Monfardini, S., Cappuzzo, F., Olmeo, N., Durando, A., Puglisi, F., Nicoletto, O., Lambiase, A. & Del Mastro, L. 2006. Multicenter phase II study of trastuzumab in combination with epirubicin and docetaxel as first-line treatment for HER2-overexpressing metastatic breast cancer. *Breast cancer research and treatment,* 95**,** 45-53.

Vokes, M. S. & Carpenter, A. E. 2008. Using CellProfiler for automatic identification and measurement of biological objects in images. *Curr Protoc Mol Biol,* Chapter 14**,** Unit 14 17.

Vuong, D., Simpson, P. T., Green, B., Cummings, M. C. & Lakhani, S. R. 2014. Molecular classification of breast cancer. *Virchows Arch,* 465**,** 1-14.

Wang, B., Lau, Y. Y., Liang, M., Vainshtein, I., Zusmanovich, M., Lu, H., Magrini, F., Sleeman, M. & Roskos, L. 2012. Mechanistic Modeling of Antigen Sink Effect for Mavrilimumab Following Intravenous Administration in Patients With Rheumatoid Arthritis. *The Journal of Clinical Pharmacology,* 52**,** 1150-1161.

Wang, J., Lei, M. & Xu, Z. 2021. Aberrant expression of PROS1 correlates with human papillary thyroid cancer progression. *PeerJ,* 9**,** e11813.

Wang, Y., Moncayo, G., Morin, P., Jr., Xue, G., Grzmil, M., Lino, M. M., Clement-Schatlo, V., Frank, S., Merlo, A. & Hemmings, B. A. 2013. Mer receptor tyrosine kinase promotes invasion and survival in glioblastoma multiforme. *Oncogene,* 32**,** 872-82.

Weigelt, B., Peterse, J. L. & van 't Veer, L. J. 2005. Breast cancer metastasis: markers and models. *Nat Rev Cancer,* 5**,** 591-602.

Weiner, G. J. 2010. Rituximab: mechanism of action. *Semin Hematol,* 47**,** 115-23.

Werfel, T. A., Elion, D. L., Rahman, B., Hicks, D. J., Sanchez, V., Gonzalez-Ericsson, P. I., Nixon, M. J., James, J. L., Balko, J. M., Scherle, P., Koblish, H. K. & Cook, R. S. 2018. Treatment-induced tumor cell apoptosis and secondary necrosis drive tumor progression in the residual tumor microenvironment through MerTK and IDO-1. *Cancer Res*.

White, K. F., Rausch, M., Hua, J., Walsh, K. H., Miller, C. E., Wells, C. C., Moodley, D., Lee, B. H., Chappel, S. C., Holland, P. M. & Hill, J. A. 2019. Abstract 558: MERTK-specific antibodies that have therapeutic antitumor activity in mice disrupt the integrity of the retinal pigmented epithelium in cynomolgus monkeys. *Cancer Research,* 79**,** 558.

World-Cancer-Research-Fund 2018. Diet, nutrition, physical activity and breast cancer.

Yan, D., Parker, R. E., Wang, X., Frye, S. V., Earp, H. S., 3rd, DeRyckere, D. & Graham, D. K. 2018. MERTK Promotes Resistance to Irreversible EGFR Tyrosine Kinase Inhibitors in Non-small Cell Lung Cancers Expressing Wild-type EGFR Family Members. *Clin Cancer Res,* 24**,** 6523-6535.

Yoshida, K., Fujikawa, T., Tanabe, A. & Sakurai, K. 1993. Quantitative analysis of distribution and fate of human lung cancer emboli labeled with 125I-5-iodo-2'-deoxyuridine in nude mice. *Surg Today,* 23**,** 979-83.

Zahavi, D., AlDeghaither, D., O'Connell, A. & Weiner, L. M. 2018. Enhancing antibody-dependent cell-mediated cytotoxicity: a strategy for improving antibody-based immunotherapy. *Antibody Therapeutics,* 1**,** 7-12.

Zhang, Y., Li, D., Jiang, Q., Cao, S., Sun, H., Chai, Y., Li, X., Ren, T., Yang, R., Feng, F., Li, B. A. & Zhao, Q. 2018. Novel ADAM-17 inhibitor ZLDI-8 enhances the in vitro and in vivo chemotherapeutic effects of Sorafenib on hepatocellular carcinoma cells. *Cell Death Dis,* 9**,** 743.

Zhou, Y., Fei, M., Zhang, G., Liang, W. C., Lin, W., Wu, Y., Piskol, R., Ridgway, J., McNamara, E., Huang, H., Zhang, J., Oh, J., Patel, J. M., Jakubiak, D., Lau, J., Blackwood, B., Bravo, D. D., Shi, Y., Wang, J., Hu, H. M., Lee, W. P., Jesudason, R., Sangaraju, D., Modrusan, Z., Anderson, K. R., Warming, S., Roose-Girma, M. & Yan, M. 2020a. Blockade of the Phagocytic Receptor MerTK on Tumor-Associated Macrophages Enhances P2X7R-Dependent STING Activation by Tumor-Derived cGAMP. *Immunity*.

Zhou, Y., Yao, Y., Deng, Y. & Shao, A. 2020b. Regulation of efferocytosis as a novel cancer therapy. *Cell Communication and Signaling,* 18**,** 71.

Zizzo, G. & Cohen, P. L. 2018. Antibody Cross-Linking of CD14 Activates MerTK and Promotes Human Macrophage Clearance of Apoptotic Neutrophils: the Dual Role of

CD14 at the Crossroads Between M1 and M2c Polarization. *Inflammation,* 41**,** 2206-2221.

Zizzo, G., Hilliard, B. A., Monestier, M. & Cohen, P. L. 2012. Efficient clearance of early apoptotic cells by human macrophages requires M2c polarization and MerTK induction. *J Immunol,* 189**,** 3508-20.

10 Acknowledgements

With this finished work, I sincerely thank all involved people who have supervised, supported and accompanied me on this journey of acquiring my doctoral degree.

First and foremost, I would like to express my gratitude to Prof. Klaus Pantel MD for supporting my endeavors to conduct my research in the United States and Prof. Sohail Tavazoie MD PhD for giving me the opportunity of being a visiting student in his laboratory. Learning from Prof. Tavazoie in weekly meetings has given me a deeper understanding of medical research and science in general.

I would like to thank Benjamin Ostendorf MD PhD for being my mentor, friend and colleague. Ben inspired me not only with his kind personality but especially with his strong motivation for excellency and his strong conviction to improve the world with his research work. The long days together in the lab, stimulating evening discussions at the bench or relaxing lunch breaks in New York City will remain as very special memories to me.

I am grateful about the entire Tavazoie lab for their warm mentoring and constant support. Special acknowledgment goes to several hundred mice, that were sacrificed for the conduction of the experiments. Furthermore, I thank Prof. Martin Horstmann MD PhD for providing the opportunity to learn research methodologies in his laboratory as a preparation for this research.

I also thank the *Studienstiftung des deutschen Volkes*, *Rockefeller University* and the *Tavazoie Lab* for financially supporting my thesis.

My extraordinary thanks go to my friends. They have given me the motivation and perseverance to complete my dissertation through their constant support and encouragement.

Special thanks go to my parents, who made my life possible so far and who never stopped believing in and supporting me.

Lastly, I would like to thank Jesus Christ for saving my life, giving me guidance and wisdom.

11 Curriculum Vitae

For privacy reasons, the Curriculum Vitae is not included in the online version.

12 Statutory Declaration

Eidesstattliche Versicherung

Ich versichere ausdrücklich, dass ich die Arbeit selbständig und ohne fremde Hilfe verfasst, andere als die von mir angegebenen Quellen und Hilfsmittel nicht benutzt und die aus den benutzten Werken wörtlich oder inhaltlich entnommenen Stellen einzeln nach Ausgabe (Auflage und Jahr des Erscheinens), Band und Seite des benutzten Werkes kenntlich gemacht habe.
Ferner versichere ich, dass ich die Dissertation bisher nicht einem Fachvertreter an einer anderen Hochschule zur Überprüfung vorgelegt oder mich anderweitig um Zulassung zur Promotion beworben habe.
Ich erkläre mich einverstanden, dass meine Dissertation vom Dekanat der Medizinischen Fakultät mit einer gängigen Software zur Erkennung von Plagiaten überprüft werden kann.

Unterschrift: .....